Seminar Proceedings

Engineering Excellence: Simulation for Fatigue Strength and Durability

Seminar Sponsors

ISBN 978-1-83979-238-0

THE INTERNATIONAL ASSOCIATION FOR THE ENGINEERING MODELLING, SIMULATION, AND ANALYSIS COMMUNITY.

ORGANIZED BY

NAFEMS

THE INTERNATIONAL ASSOCIATION FOR THE ENGINEERING
MODELLING, SIMULATION, AND ANALYSIS COMMUNITY.

ISBN 978-1-83979-238-0

Contents

Hybrid System Simulation: New Trends and Methods in Vehicle Engineering

Michael Burger (Fraunhofer ITWM)

1 Summary

In this contribution, we give an overview on current developments, new trends and challenges in the field of vehicle engineering. This includes both the application topic perspective, and the methodological side as well. We start with a review and summary of classical mathematical methods for computer-aided engineering (CAE) of vehicles, which built a dedicated backbone for many modern techniques. In particular, in the considered automotive field, the availability of data has been increasing strongly for years; this applies not only to quantities measured directly on a vehicle, but also to information and data describing the environment. At the same time, technologies for data acquisition, data management, communication and computational data processing are also continuously improved and further developed. Today, both allow to derive more and more valuable knowledge and information from existing data sets using suitable methods and tools from data-based mathematics. Moreover, the combination of classical system simulation with data analytics and methods and tools from artificial intelligence (AI) reveal the potential to significantly improve different stages in the vehicle development process.

We reflect all these methodological trends and potentials in the context of classical mechanical engineering for vehicle design and development and consider additional, new application topics: new drivetrain technologies, resource efficiency and automated vehicles, driver assistance systems and autonomous driving functions (ADAS/AD) [1,4,5].

We discuss and highlight the new trends and combinations on the basis of selected engineering examples:

- AI methods in vehicle engineering: Identification of usage profiles with vehicle field-monitoring data and derivation of highly efficient surrogate models [1,6].
- Derivation of customer- and region-specific durability loads and energy demands for modern vehicles, on the basis of geographic data and simulation models [1].
- Virtual environments and system simulation for (interactive) driving scenarios [2,3].

We illustrate these application examples; we discuss the properties of the underlying mathematical models and tools and we address, in particular, the corresponding optimal model complexity for specific tasks and targets.

2 References

[1] M. Burger, K. Dreßler, M. Speckert: Load assumption process for durability design using new data sources and data analytics. International Journal of Fatigue 145, Art. 106116, 425–432, 2021.

[2] M. Burger, T. Jung, C. Wu, T. Rothmann: Umgebungsdaten und Dynamische Verkehrsszenarien zur Effizienten Erprobung von Fahrzeug-Systemen. VDI-Bericht 2407, 2022, S. 423-436.

[3] T. Rothmann, J. Schwank, J. Frank, M. Burger: Multiskalen-Generierung von virtuellen Szenen und Szenarien zur Entwicklung, Erprobung und Validierung von Funktionen für autonome Fahrzeuge. VDI-Bericht 2436, 2024, S. 161-174

[4] M. Burger: Daten, Künstliche Intelligenz und Maschinelles Lernen in der Fahrzeugentwicklung. Mitteilungen der Deutschen Mathematiker-Vereinigung, Band 30, Heft 3, 2022.

[5] J.-P. Kobler, A. Brand, S. Weßel, T. Jung, S. Steidel, M. Burger: Online-Identifikation von Straßenrauigkeiten am LKW-Trailer für sicheres autonomes Fahren. In: Berns, K., Dressler, K., Kalmar, R., Stephan, N., Teutsch, R., Thul, M. (eds) Commercial Vehicle Technology 2022, pp. 210-225, Springer Vieweg, Wiesbaden (2022).

[6] M. Burger, J. Fiedler, M. Jansen, J. Kickertz, V. Kleeberg, A: Philippi: Vehicle activity recognition using machine data. Proceedings of the 8th International Commercial Vehicle Technology Symposium 2024, Kaiserslautern – to appear.

Fatigue Strength Assessment of Fiber-Reinforced Plastic Components with Standard Material Data

M. Stojek, S.Pazour (PART Engineering),
V. Mortazavian (Ascend Performance Materials)

1 Motivation

The use of plastic components in technical applications, especially in the automotive sector, has always required developers to evaluate the service life under oscillating loads. With the increasing substitution of metals, this requirement is growing. At the same time, the number of available material types is increasing due to optimized properties, adapted to special requirements. The measurement of characteristic values for the fatigue strength (SN-curves) is expensive and time consuming, not least because of the relatively low permissible frequencies for plastics under vibrating loads due to their self-heating.

An *anisotropic* fatigue assessment increases the necessary amount for measurement data considerably due to the directional dependency, making anisotropic SN-curves a rare resource. Therefore, estimating or simplifying methods are very helpful for fatigue assessment and are often the only option for a simulation driven design.

2 Approach

Ascend has developed a group of fiber reinforced PA66 grades with particularly good damping properties. While improving the components performance, higher damping in general reduces the allowable testing frequency even more.

A special test component has been tested in static and cyclic loading conditions. (although investigated, NVH and acoustics are not covered here). Figure 1 shows the test component used in the structure for vibrational stress.

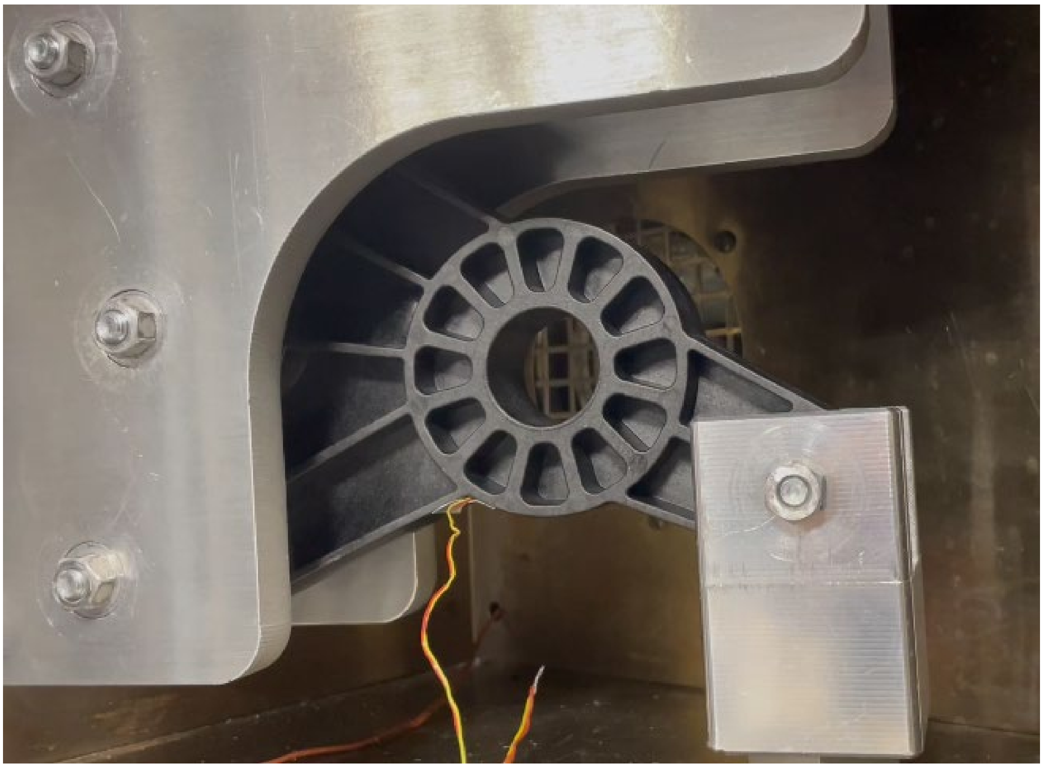

Figure 1 Test Component Under Cyclic Loading

In a first approach, a fatigue assessment is presented based on an isotropic simulation and the Oberbach method [1]. Generic Wöhler curves are generated based on short-term tensile tests (see Fig. 2) and local utilization ratios are calculated. In an additional step, an anisotropic procedure based on these generic SN curves is discussed. This includes an anisotropic material model for the stress calculation and the components stiffness.

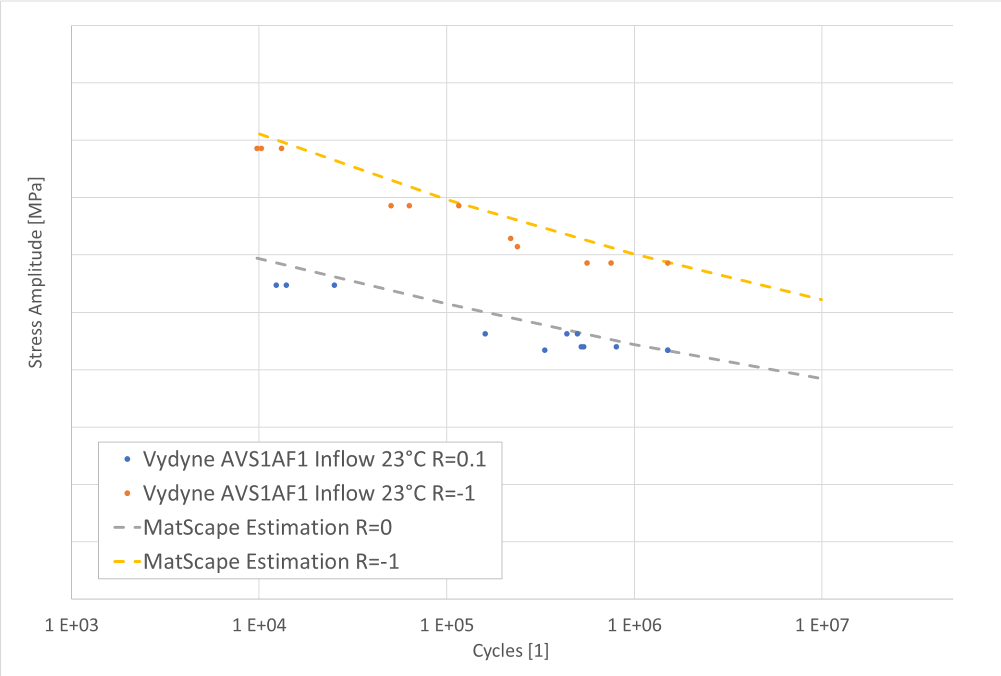

Figure 2 Comparison Between Measured Data and Generic SN-Curves

All calculation results are compared with the real test data.

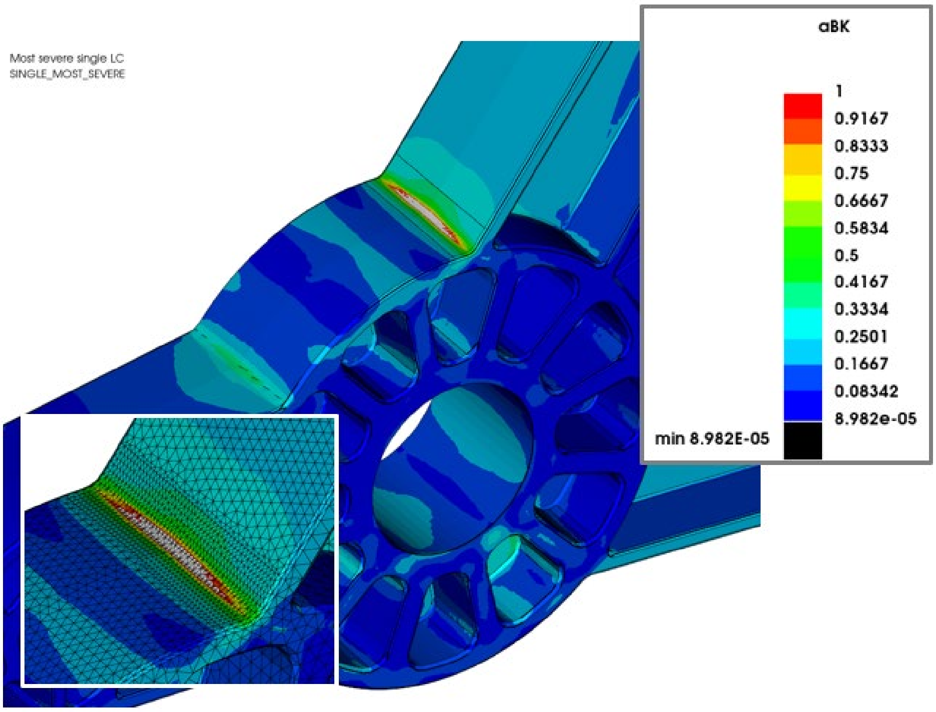

Figure 3 Result of a Fatigue Assessment with S-Life Plastics

3 References

[1] Reprint (10/2020): Allowable Strength Limits, Kunststoffe, Oberbach, www.partengineering.com

Durability And Damage Tolerance (DADT) of AM Components

Ramesh Chandwani, Chris Timbrell

Zentech International Limited

Summary

With ever increasing use of AM components, Cold Spray AM (CSAM) parts and Cold Spray Repairs used in Aerospace industry which may contain minute sized discontinuities, a number of International Standards Organisations have stated that for the Certification purposes, Durability and Damage Tolerance (DADT) analysis based on linear elastic fracture mechanics (LEFM) principles is mandatory. In this presentation the authors have described how this this has been achieved in FE based software based on small crack propagation law.

Background

In Defence and Aerospace industries use of AM components and adhesively connected repair plates has increased, especially since 2019, with the approval of US authorities to improve operation supply chains and logistic resiliency. Both the US MIL-STD-1530D [1] and NASA Fracture Control Handbook NASA-HDBK-5010 [2] also mandate that requisite level of qualification, certification and risk/safety evaluation must be carried out by an appropriate engineering support activity based on Linear Elastic Fracture Mechanics (LEFM) principles and perform predictive Durability and Damage Tolerance (DADT) assessment for all AM parts/repair patches.

This paper describes how a general crack grow simulation approach can be used with a modified Hartman-Schijve crack growth law which is applicable for short and long crack regimes. Examples are provided to show how multiple sets of test data can be collapsed to a unified single curve when using this form of crack growth law. Simulation examples are also provided.

References

[1] MIL-STD-1530D (W/ CHANGE-1), Department Of Defense Standard Practice: Aircraft Structural Integrity Program (ASIP) (13 Oct 2016). Available online: http://everyspec.com/MIL-STD/MIL-STD-1500-1599/MIL-STD-1530D_CHG-1_55391

[2] NASA-HDBK-5010, Fracture Control Handbook For Payloads, Handbook For Payloads, Experiments, And Similar Hardware (19 Oct 2017). Available online : https://standards.nasa.gov/standard/nasa/nasa-hdbk-5010

Structural Integrity from the Past to the Future

Michel Guillaume

Centre for Aviation; Zurich University of Applied Sciences ZHAW

Summary of Presentation

In the early days of powered aviation, aircraft were designed for purely static conditions. From 1940 onwards, more and more the safe life structural design philosophy was adopted that gave due consideration to material fatigue from flight cycles. The failsafe design philosophy with multiple load paths and crack stoppers was intended to provide more safety. But the two crashes of the De Havilland Comet, the first jetliner, after only about 1'000 cycles highlighted the need for structural testing to ensure a safe structure throughout the whole service life of an aircraft. For the first Boeing 707 and Douglas DC-8 aircraft, the structure was improved based on findings from the Comet disasters – for example by introducing a new window design and crack stoppers in the fuselage and applying aluminum 2024-T3 for the skins. The crash of a US Air Force F-111 Bomber with only 107 flight hours in 1969 triggered a further, important research activity to reconceptualize structural integrity, which developed into the fatigue design philosophy of damage tolerance. Damage tolerance assumes an initial discontinuity from material or manufacturing. Subsequently, from the first flight hour crack propagation starts until eventually it leads to failure. In the 1970, the US AIR FORCE introduced an aircraft structural integrity plan (ASIP) with five phases (tasks, details see figure 1):

- Design Information
- Design Analysis and Development Tests
- Full Scale Testing
- Force Management Data Package
- Force Management

Full-Scale Development			Force Management	
Task I Design Information	Task II Design Analyses & Development Testing	Task III Full Scale Testing	Task IV Certification & Force Management Development	Task V Force Management Execution
ASIP Master Plan Design Service Life and Design Usage Structural Design Criteria Durability & Damage Tolerance Control Program Corrosion Prevention and Control Program Nondestructive Inspection Program Selections of Materials, Processes, Joining Methods & Structural Concepts	Material and Joint Allowables Loads Analysis Service Loads Spectra Chemical/ Thermal Environment Spectra Stress Analysis Damage Tolerance Analysis Durability Analysis Corrosion Assessment Sonic Fatigue Vibration Analysis Mass Properties Analysis	Static Tests First Flight Verification Ground Tests Flight Tests Durability Tests Damage Tolerance Tests Climatic Tests Interpretation & Evaluation of Test Results	Certification Analyses Strength Summary And Operating Restrictions Force Structural Maintenance Plan Loads/Environment Spectra Survey Methodology Individual Airplane Tracking Program Methodology Individual Aircraft Tracking Program Development	Individual Airplane Tracking Data Loads/Environment Spectra Survey ASIP Manual Aircraft Structural Records Force Management Updates Recertification

Figure 1: Detail activities of the ASIP masterplan

Today, the damage tolernace structural design philosophy has become a standard even in civil aviation. All primary structures must be designed and tested for damage tolerance requirements. The Aloha incident of a Boeing 737 in 1978 showed that additionally wide spread fatigue damage must be

considered. All of the large aircraft manufacturers, such as Airbus, Boeing, and McDonnell Douglas had to perform intensive supplemental inspection programs to maintain the safety of flight. Since 2011, all civil CS25 or FAR25 aircraft have to be tested for up to three times their design life without sustaining any widespread fatigue damage. This requirement is referred to the demonstration of the limit of validity.

Another example that highlights the importance of ongoing fatigue monitoring is that of the Jet fighters in the Swiss Military, which experienced severe fatigue damages early on in life of the aircraft. At 1’000 flight hours the Mirage III already showed severe cracks in some of the holes of the main spar. In the full scale fatigue test that had been conducted in Switzerland, three main spars failed after between 4’800 and 7800 flight hours without fulfilling the test life of 20’000 flight hours to demonstrate the service life of 4’000 flight hours (safety factor of 5 was applied for safe life philosophy). All spars of the Swiss Mirage III fleet were replaced by a redesigned main spar which was approved in the full-scale fatigue test of 1’200 flight hours of in-service usage.
Based on experience, the Swiss Military requested during the procurement of the F/A-18 to perform a detailed structural analysis based on the US AIR FORCE ASIP master plan. The structure of the center fuselage section needed to be reinforced by titanium bulkheads and required a redesign of the most critical locations in the center fuselage and the wing structure to demonstrate a service life expectancy for the Swiss F/A-18 of 5’000 service flight hours. This redesign was qualified by a full scale fatigue test, based on the advanced test technology of IABG in Emmen at Ruag Aerospace, which ran from January 2003 to September 2004, see figure 2.

Figure 2: Swiss full scale fatigue test with efficient test set-up with tree inspection platforms

For loads development, which are an important task for the structural design, artificial intelligence (AI) will be big help for computational fluid dynamics simulations in future. With reinforced learning, the mesh and quality of results can be improved from run to run, which will increase the speed of obtaining results from simulations. Combining this with wind tunnel data, the number of tests can be further reduced and optimized to develop the loads for aircraft design. If data form previous projects can be used, the use of AI will be even more powerful. In general, AI can provide major benefits in all simulation disciplines, such as finite element analysis, aeroelastic calculation and fatigue analysis including testing of materials.

Today, aircraft structures for primary structures are complex, with different materials of metals, carbon fiber, reinforced plastics, or hybrid structures Therefore, not only variable amplitude stress cycles play an important role but also thermal cycle stresses must be considered. The fatigue and damage behavior of metals, fiber metals, carbon fiber reinforced plastics are very different and require a lot of testing along the test pyramid (building block approach). The trend is to replace physical testing by virtual testing using simulations or a mix of physical and virtual testing, which is referred to as a hybrid test pyramid, see figure 3. Further, the use of artificial intelligence AI will reduce the effort of physical testing and allow optimized testing to save time and cost. The huge materials and structural data generated over the last 50 years processed with AI methods could bring a lot of efficiency for structural aircraft design. Data from service experience would be a big help, but so far, only the Military uses structural health monitoring for managing individual aircraft. Structural health monitoring systems using strain gauges with a data acquisition system are complex absorb a lot of resources. This has a cost impact because the system also needs maintenance to keep it operational over a long time (20 to 30 years of service). In the civil world of airliners, any equipment which is not mandatory will not be considered due to costs and efficient daily operation of the aircraft. The heavy maintenance of airliners must be planned well ahead for the fleet management. An individual structural aircraft tracking for doing inspection based on structural life consumed is not yet considered as practical.

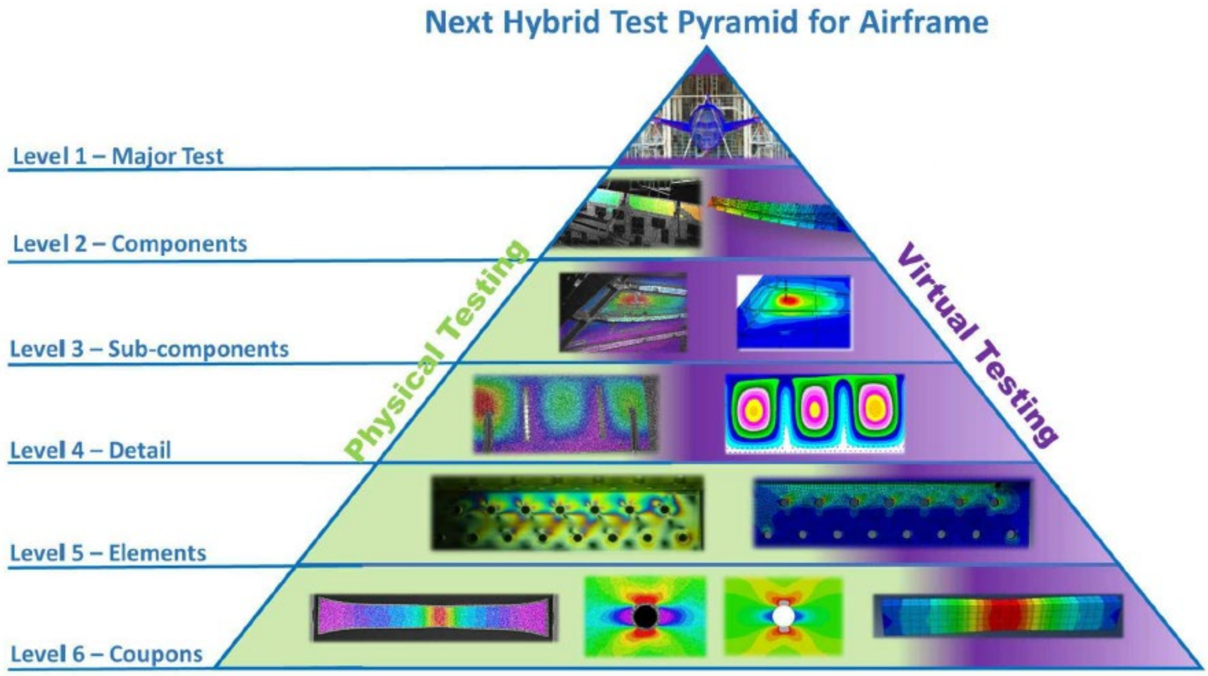

Figure 3: Test pyramid for physical and virtual testing

The concept of having a Digital Twin is appealing to manage all the systems over the whole life cycle and allows maintenance based on conditions inspections and part replacement of the aircraft. But to keep such a system running with a lot of design and operational data from sensors, the need for energy and resources is quite high. For the US AIR FORCE the effort is too big to maintain for every aircraft system a Digital Twin. Every manufacturer uses different hardware and software systems, which is not cost effective at all.
In the civil world most airlines do not want to provide their operational data to the manufacturers or to an independent maintenance organization, which is a real drawback for the use of the full potential of Digital Twin.

Using AI technology in aviation for aircraft design and operation has several challenges. Due to high safety standards with a very high reliability, processes for verification and validation must be established. This must be done in collaboration with the aviation authorities, such as the FAA and EASA. Eventually, digital technology will need to be certified. An important question is the right size approach for the application of digital technology when using AI. To make progress in this fast-growing field the aviation, stake holders need to work close together. This must be an international effort. A first step would be to bring together all the AI road maps from authorities, manufacturers, maintenance companies, and the airline industry to develop a realistic and feasible road for the next 10 years.

A lot of testing will be needed to train current and future simulation tools for the development of new sustainable aircraft. AI technology may be helpful to improve and increase the analysis of the huge amount of data.

Crack Propagation Modelling for Fatigue Analysis

Filip Van den Abeele (subseawolf)

1 How to Simulate Crack Propagation using Finite Element Analysis

To simulate fatigue crack growth in engineering structures, the finite element method offers different possibilities, such as:

- **Constitutive Material Modelling (CDM)**
  In this approach, inspired by the theory of Continuum Damage Mechanics (CDM), the onset of (fatigue) crack growth is governed by a damage initiation criterion. After damage initiation, the elastic material stiffness is degraded progressively according to a specified damage evolution response. Upon reaching maximum degradation, the failed elements are removed from the mesh, hence reflecting progressive (fatigue) crack growth. The CDM approach to fatigue crack propagation is a well-developed scientific topic, and a comprehensive overview can be found in e.g. [1].

- **Cohesive Zone Models (CZM)**
  A cohesive zone model idealizes the fracture process in solids as occurring within thin layers confined by two adjacent virtual surfaces. The loss of cohesion within a solid, and thus (fatigue) crack formation and extension, is viewed as the progressive decay of otherwise intact tension and shear stresses across adjacent surfaces. The introduction of an interface constitutive law, connecting tractions and displacements, provides a description for the progressive (fatigue) fracture. A cohesive zone model allows for separation of interfaces between continuum elements if some critical value of separation is reached locally, whereas the material outside deforms according to the imposed constitutive material law without any damage. The use of cohesive zone modelling to simulate fatigue crack propagation is described in a.o. [2].

- **Virtual Crack Closure Techniques (VCCT)**
  The Virtual Crack Closure Technique is based on the assumptions that the strain energy released when a crack is extended by a certain amount is the same as the energy required to virtually close the crack by the same amount. The VCCT criterion is based on the principles of Linear Elastic Fracture Mechanics (LEFM), and hence appropriate for problems where (quasi-) brittle crack propagation occurs along predefined crack paths. For a good introduction to the VCCT approach and its application, the interested reader is referred to [3].

- **Extended Finite Element Method (XFEM)**
  XFEM is an extension of the conventional finite element method based on the concept of partition of unity, which allows local enrichment functions to be easily incorporated into an FE approximation. The presence of discontinuities is ensured by special enriched functions in conjunction with additional degrees of freedom. As a consequence, XFEM can be used to simulate (fatigue) crack initiation and propagation along an arbitrary, solution-dependent path, since the crack growth is not tied to the element boundaries in the mesh. An application of XFEM to simulate three-dimensional fatigue crack growth in engineering components is found in [4].

NAFEMS has published both a primer on the use of fracture mechanics methods in finite element analysis [5] and an extensive textbook on Crack Propagation Modelling [6]. This paper highlights two examples from the latter publication, explaining the use of special modelling techniques to simulate fatigue crack propagation. In the first example, the use of XFEM to simulate fatigue crack growth in a gas compressor turbine disc is discussed. The second example covers both XFEM and CZM to calculate stress intensity factors and predict fatigue crack growth in a complicated helicopter component. Both examples demonstrate how crack propagation modelling can be applied for fatigue analysis of engineering components.

2 Fatigue Crack Growth in a Gas Compressor Turbine Disc

As an example of the use of the Extended Finite Element Method (XFEM) for fatigue analysis, we highlight crack growth modelling for a gas compressor turbine disc of an aircraft engine, documented in [7 – 8]. In aircraft engines, the turbine discs are safety-critical components as they are susceptible to fatigue crack propagation, e.g. emanating from tie bolt holes. During aircraft engine operation, these rotating discs are subjected to biaxial loading conditions which have a significant influence on the fatigue crack growth rate [9]. Kumar et al. have applied an XFEM-based numerical scheme to predict fatigue crack growth in aircraft engine turbine discs made of Ni-based alloy [7 – 8]. They studied a disc of 250 mm diameter with four bolt holes (with diameter of 5 mm) in the web portion. A quarter model of the turbine disc is shown in Figure 1, also indicating the dimensions and the finite element mesh:

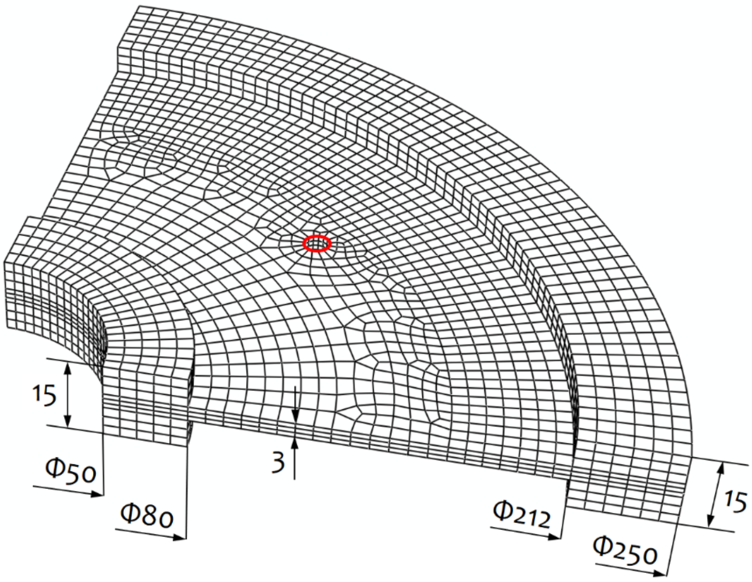

Figure 1: Gas Compressor Turbine Disc – Geometry and Mesh

An initial crack with length $a_0 = 0.9$ mm is assumed at the periphery of the bolt hole. A constant amplitude cyclic load with amplitude $\Delta\sigma = 100$ MPa and stress ratio $R = 0.1$ is applied at the outer surface of the rim. The equivalent stress intensity factor range ΔK_{eff} is computed from the J-integral, which is then used in the Paris law

$$\frac{da}{dN} = C\left(\Delta K_{eff}\right)^m \tag{1}$$

to calculate the fatigue crack growth rate.

Table 1: Properties of Nickel Based Super Alloy [7]

		$T = 26°C$	$T = 650°C$
E	[GPa]	184.5	180
ν	[-]	0.33	0.33
σ_y	[MPa]	780	653
σ_u	[MPa]	1 014	987
C	[-]	2.82 e^{-10}	1.78 e^{-8}
m	[-]	3.95	2.89
M	[-]	3.3884 e^{-15}	
α	[-]	6.10	
β	[-]	3.68	

Since the gas compressor turbine is operating at elevated temperatures, the material properties for the Nickel based super alloy, summarized in Table 1, are taken for $T = 650℃$. The fatigue crack growth curve predicted by XFEM, shown in Figure 2, is consistent with the theoretical expectation for a Paris-type Stage II law.

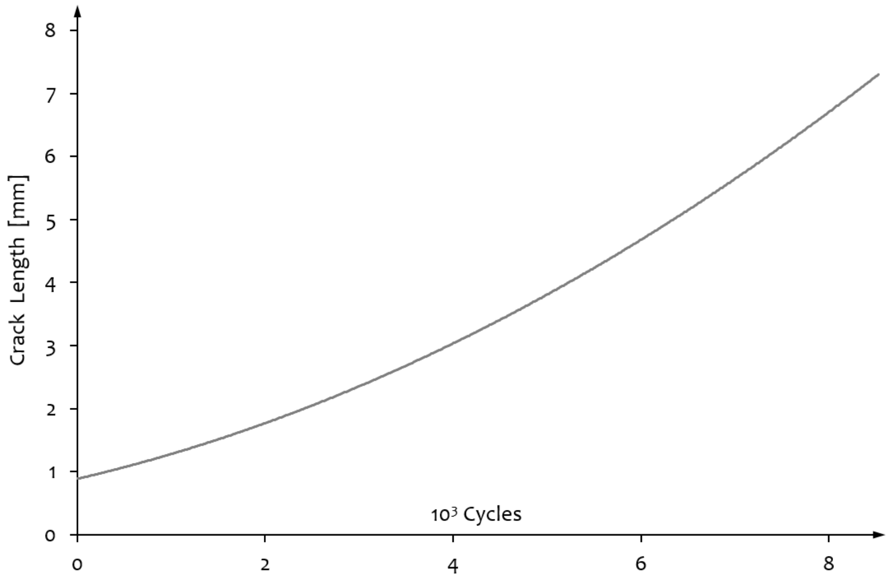

Figure 2: Predicted Fatigue Crack Growth in Gas Compressor Turbine Disc

The XFEM fatigue analysis presented here is based on the conventional Paris law for the stage II fatigue crack growth rate. Pandey [8] has also performed a high cycle fatigue analysis of the turbine disc using a damage law

$$\frac{dD}{dN} = M \, \frac{1 - \exp\,(-\alpha)}{\alpha} \, \left(\sigma_{max}^{eq} - \sigma_{min}^{eq}\right)^{\beta} \exp(\alpha D) \; R_{\eta}^{\beta/2} \tag{2}$$

where $\{M, \alpha, \beta\}$ are material constants with the values shown in Table 1, σ_{max}^{eq} and σ_{min}^{eq} are the maximum and minimum equivalent stresses respectively, and

$$R_{\eta} = \frac{2}{3} \, (1 + \nu) + 3(1 - 2\nu)\eta^2 \tag{3}$$

is the stress triaxiality function, described by the Poisson's ratio ν and the stress triaxiality η. His analysis showed that the combination of XFEM with continuum damage mechanics can be used to predict crack growth in real life engineering problems.

A compelling advantage of finite element analysis is the ability to visualize and study the location and the extent of a propagating crack front in a complex 3D structure. Chandwani [9] used a crack block approach to study fatigue crack propagation during a spin test of a turbine engine disc. The crack block method enables the prediction of large scale crack growth in 3D bodies by allowing the crack front to move through the finite element model [10]. The predicted crack propagation path for the turbine disc spin test, assuming a Paris-type law for the fatigue crack growth rate, is shown in Figure 3 for both low-cycle and high-cycle fatigue loads:

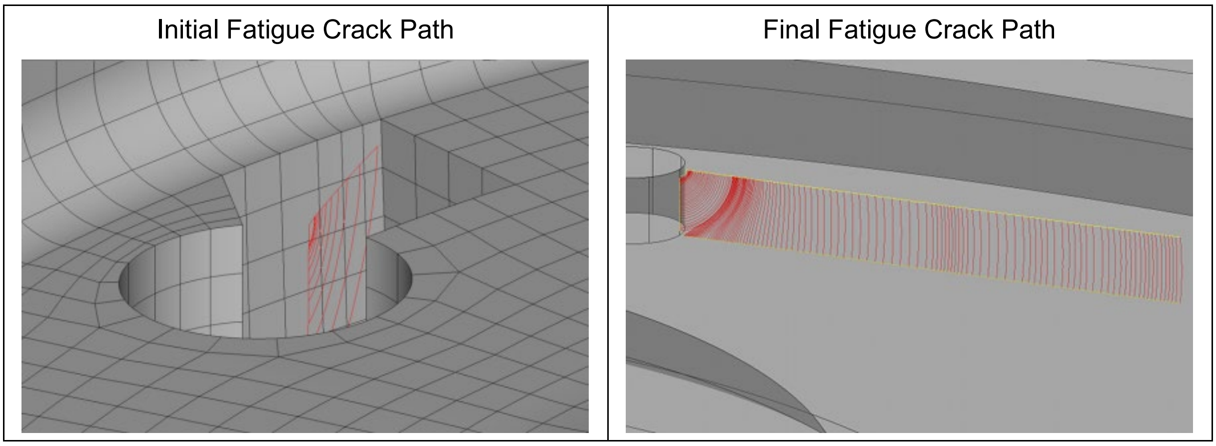

Figure 3: Prediction of Fatigue Crack Propagation in Spin Test [9]

These detailed insights in the progression of the growing fatigue crack front allow developing a more informed view on the remaining lifetime of a cracked body then a mere crack length curve $a(N)$ such as shown in Figure 2. More details on fatigue crack growth prediction in aircraft engines can be found in [7–12].

3 Fatigue Crack Growth in a Complicated Helicopter Component

As another example of crack growth modelling for fatigue analysis, we discuss a round-robin challenge problem to predict fatigue crack growth in a complex helicopter component under rotor-craft spectrum loading [13]. The benchmark problem related to a corner defect (with radius $r = 2$ mm) at the edge of a large central hole in a flanged plate made of 7010-T73651 aluminium alloy [14].

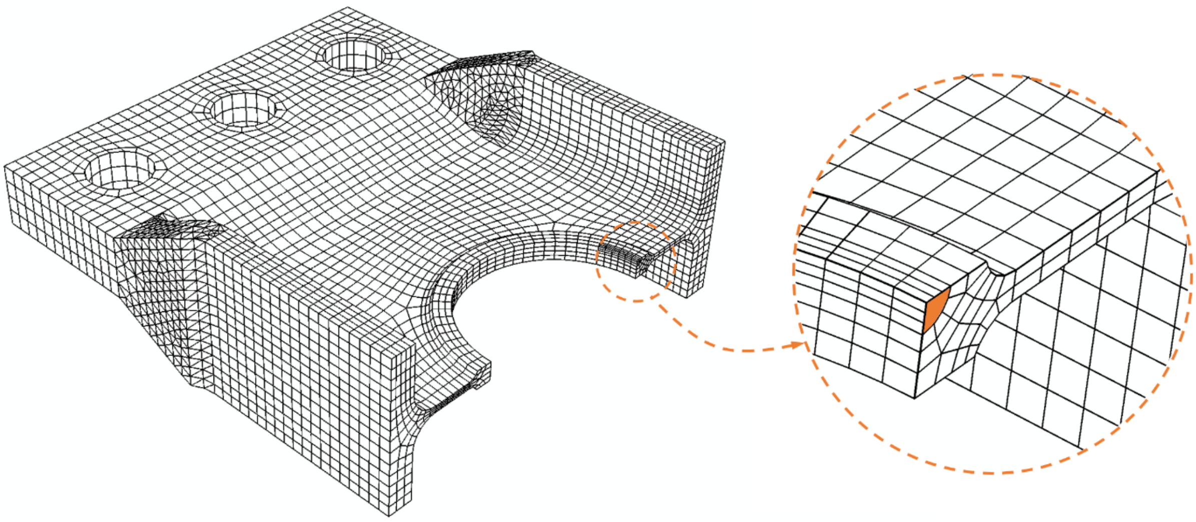

Figure 4: Finite Element Model for Helicopter Airframe Component

Figure 4 shows the symmetric finite element model for the helicopter airframe component, and a detail of the corner defect. The model contains 14 900 quadratic reduced integration 3D elements, and the initial defect and the anticipated crack front are assumed to stay in the plane of symmetry. The flanged plate was subjected to the Asterix rotorcraft spectrum, which represents 191 hours of helicopter flight and is composed of 317 610 cycles.

Figure 5 shows a cross section with the initial 2-mm corner crack. The subsequent crack-front shapes illustrate the approximate crack path as the defect grows from the corner crack to a final crack with length $a \approx 25$ mm. These experimental observations were provided by Airbus [15]. As illustrated in Figure 5, the corner flaw was located in a 6 mm thick region, and transitioned into a thin (2 mm thick) section after about 5 mm of crack growth. The crack finally propagates into an 8 mm thick flange (perpendicular to the crack direction) after 25 mm of cumulated crack growth.

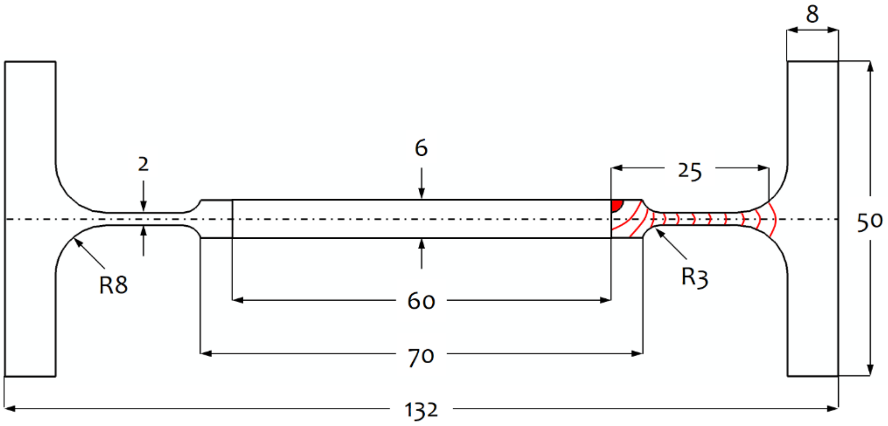

Figure 5: Fatigue Crack Propagation in Helicopter Component [13]

We have used the finite element model shown in Figure 4 to calculate stress intensity factors for different crack profiles (circular, oblique and straight) observed during the fatigue spectrum loading. The normalized stress intensity factors for these different crack types are shown in Figure 6 as a function of the normalized distance along the crack front:

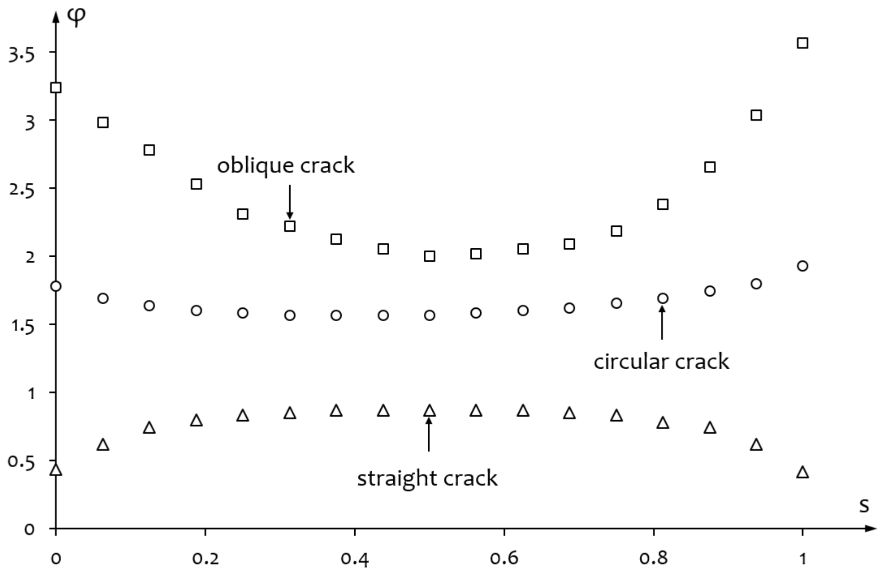

Figure 6: Stress Intensity Factors for Different Crack Shapes and Lengths

The results shown in Figure 6 are in line with the values published by Irving [8], who used the BEASY boundary element code; and Shi [11], who used XFEM to calculate stress intensity factors for different three-dimensional crack configurations:

- The initial corner crack has a (quarter) circular shape with a radius of $r = 2$ mm. The normalized stress intensity factor for the initial crack is shown with circles in Figure 6. The stress intensity factor for this problem shows the expected variation along the crack front, with higher values at the free surfaces. This pattern reflects the initial stages of crack growth.

- During the transition from the 6 mm section to the thin (2 mm) rim, the crack morphs into an oblique shape as schematically shown in Figure 5. The squares in Figure 6 represent the variation of the normalized stress intensity factor for an inclined crack with length $a = 6.5$ mm (measured along the free surface). Large variations in stress intensity factor are observed in this transitional range.

- When the crack propagates through the 2 mm thin section, the crack front becomes straight and the variations in stress intensity factor along the crack profile reduce. The triangles in Figure 6 show the stress intensity factors when the crack has grown into the fillet region of the edge flange. A straight crack front was assumed, and the final crack length was $a = 25$ mm (cf. Figure 5). This pattern is representative for the final stages of crack growth.

To study crack propagation in the helicopter component under *static* loading, we perform cohesive zone modelling of the component shown in Figure 4 subjected to a remote force of 100 kN. A layer of 8-node three dimensional cohesive elements was added to the symmetry plane (excluding the shape of the initial defect). The elastic properties of the 7010-T73651 aluminium alloy were chosen as $E = 70$ GPa and $\nu = 0.33$. The material has a yield stress of $\sigma_y = 434$ MPa and an ultimate tensile strength of $\sigma_u = 510$ MPa. The cohesive properties were selected as $G_c = 17$ N/mm and $T_c = 690$ MPa.

When simulating the response of the helicopter component under static loading with this cohesive zone model, crack initiation occurs at 22% of the applied load. The evolution of the predicted crack front is shown in Figure 7 for different load levels. These results confirm that a cohesive zone model can capture the subsequent profiles of a growing crack in a complex component, even with a fairly coarse mesh.

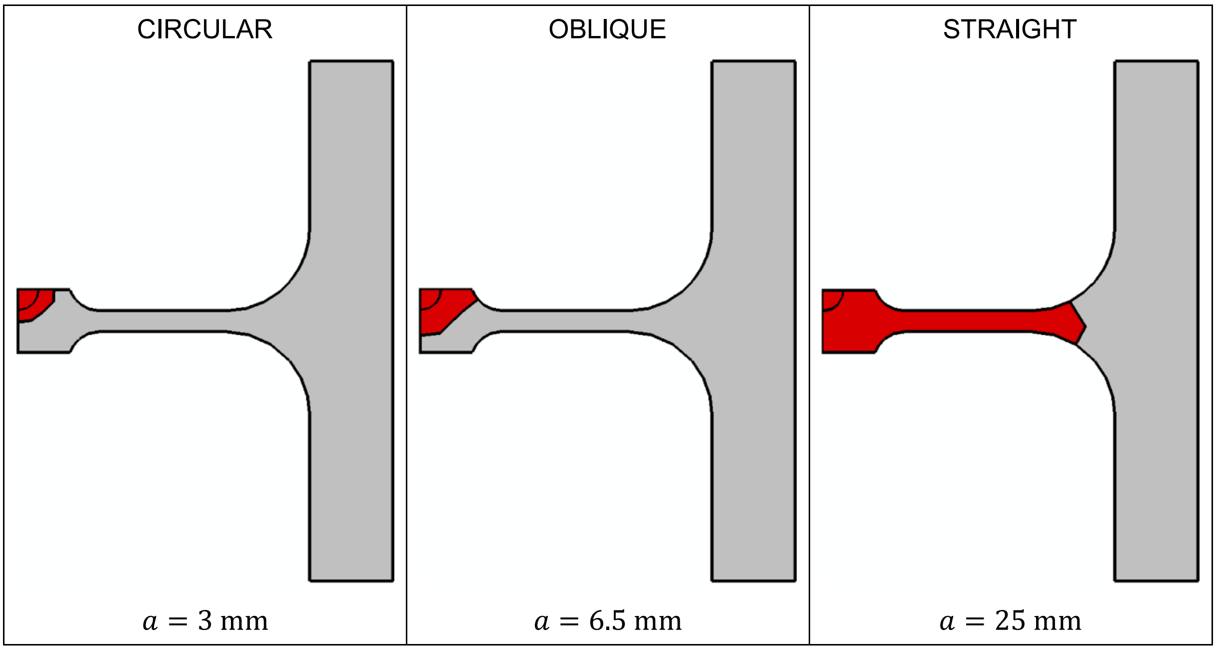

Figure 7: Evolution of the Crack Front under Static Loading

Fatigue crack propagation under rotorcraft spectrum loading is discussed in more detail in [12-16]. These authors use the AFGROW code, originally developed by the U.S. Air Force Research Laboratory, to perform fatigue life predictions and to calculate the crack length as a function of flight time. The predictions agreed very well with experimental data during the early stages of crack growth. However, the models predicted faster crack growth in the thin (2 mm) section, leading to an underestimation of the total fatigue life with ca. 30%. The authors conclude that the prediction of crack growth in helicopters, unlike fixed wing aircrafts, requires accurate calculations in the near threshold regime.

4 Conclusions

Over the past decade, the use of the finite element method to solve fracture mechanics problems has matured and is finding its way to industrial applications. This paper highlighted two examples of special modelling techniques to simulate fatigue crack propagation. The first example highlighted the use of the Extended Finite Element Method (XFEM) to simulate fatigue crack growth in a gas compressor turbine disc. The second example covered both XFEM and Cohesive Zone Modelling (CZM) to calculate stress intensity factors and predict fatigue crack growth in a complicated helicopter component. Both examples convincingly demonstrate how crack propagation modelling can be applied for fatigue analysis of engineering components. For a detailed background of the different modelling techniques available to model fatigue crack initiation and propagation in finite element analysis, the interested reader is referred to the NAFEMS Text Book on Crack Propagation Modelling [6]. This flagship publication covers many other examples on fatigue analysis of engineering structures, including pressure vessels, gearboxes, pipelines and aircraft components.

5 References

[1] Chowdury P. and Sehitoglu ., *Mechanisms of Fatigue Growth – A Critical Digest of Theoretical Developments*, Fracture and Fatigue of Engineering Materials and Structures, vol. 39(6), pp. 652-674 (2016)

[2] de Andres A., Perez J.L. and Ortiz M., *Elastoplastic Finite Element Analysis of Three Dimensional Fatigue Crack Growth in Aluminium Shafts subjected to Axial Loading*, International Journal for Numerical Methods in Engineering, vol. 44(9), pp. 1267-1282 (1999)

[3] Krueger R., *Virtual Crack Closure Technique: History, Approach and Applications*, Applied Mechanics Review, vol. 57(2), pp. 109-143 (2004)

[4] Sukumar N., Chopp D.L. and Moran B., *Extended Finite Element Method and Fast Marching Method for Three Dimensional Fatigue Crack Propagation*, Engineering Fracture Mechanics, vol. 710(1), pp. 29-48 (2003)

[5] Hellen T., *How to Undertake Fracture Mechanics Analysis*, NAFEMS Publication HT18, 74 pp. (2001)

[6] Van den Abeele F., *Crack Propagation Modelling*, NAFEMS Text Book R0130, 339 pp. (2022)

[7] Kumar M., Ahmad S., Singh I.V., Rao A.V., Kumar J. and Kumar V; *Experimental and Numerical Studies to Estimate Fatigue Crack Growth Behaviour of Ni-based Super Alloys*, Theoretical and Applied Fracture Mechanics, vol. 96, pp. 604-616 (2018)

[8] Pandey V.B., Singh I.V., Mishra B.K., Ahmad S., Rao A.V. and Kumar V., *A New Framework based on Continuum Damage Mechanics and XFEM for High Cycle Fatigue Crack Growth Simulations*, Engineering Fracture Mechanics, vol. 206, pp. 172-200 (2019)

[9] Chandwani C., *The Use of Fracture Mechanics for Fatigue Life Assessment*, Proceedings of the UK NAFEMS Seminar on Current Best Practices in Fatigue Analysis using Finite Element Analysis, London, UK (2014)

[10] Beres W., Dudzinski D. and Murzionak A., *Fatigue Crack Growth Rate Evaluation in a Turbine Disc after Spin Disc Testing,* Proceedings of the 12th International Conference on Fracture, Ottowa, Canada (2009)

[11] Zhuang W.Z., *Prediction of Crack Growth from Bolt Holes in a Disc*, International Journal of Fatigue, vol. 22(3), pp. 241-25 (2000)

[12] Newman C.J., *Application of a Closure Model to Predict Crack Growth in Three Engine Disc Materials*, International Journal of Fracture, vol. 80(2-3), pp. 193-218 (1996)

[13] Newman C.J., Irving P.E., Lin J. and Le D.D., *Crack Growth Predictions in a Complex Helicopter Component under Spectrum Loading*, Fatigue and Fracture of Engineering Materials and Structures, vol. 29(11), pp. 949-958 (2006)

[14] Irving P. and Buller R., *Prediction of Fatigue Life under Helicopter Loading Spectra for Safe Life and Damage Tolerant Design*, American Society of Testing and Materials, ASTM STP 1332, pp. 727-742 (1999)

[15] Irving P., Lin J. and Bristow J., *Damage Tolerance in Helicopters: Report on the Round Robin Challenge*, Proceedings of the 59th Annual Forum of the American Helicopter Society, Phoenix, US (2003)

[16] Shi J., Chopp D., Lua J., Sukumar N. and Belytschko T., *Abaqus Implementation of Extended Finite Element Method using a Level Set Representation for Three Dimensional Fatigue Crack Growth and Life Predictions*, Engineering Fracture Mechanics, vol. 77(14), pp. 2840-2863 (2010)

Integration of System Simulations for Simple and Meaningful Fatigue Strength Testing of Substructures

Volker Landersheim (Fraunhofer Institute for Structural Durability and System Reliability LBF)

1 Summary

Increasing time and cost pressure in product development and growing complexity due to system integration pose major challenges for fatigue strength analyses. Meaningful strength tests are often only possible in the context of the complete system, which leads to costly delays in the development process. Hybrid testing methods offer a solution by enabling earlier testing of substructures with less hardware. Only the relevant parts are used as Device under Test, while the behaviour of the surrounding structure is described by numerical models and emulated in the test by active or passive test bench components. This enables an efficient combination of numerical and experimental strength assessment.

2 Introduction

The reliable design of mechanical structures regarding structural durability is a basic prerequisite for the smooth and safe use of machines and means of transport. In recent decades, numerical simulation tools have led to significant progress in the design and optimisation of strength and weight. Experimental proof of structural durability nevertheless remains largely indispensable. However, the validity of such a laboratory test is heavily dependent on the selected boundary conditions in the test, which always represent an abstraction of the actual application. This applies in particular to substructures and sub-systems that are integrated into or connected to elastic structures in a complex manner. Such substructures usually involve many internal loads and a pronounced dependence of the load condition on the elastic behaviour of the surrounding structure. As a result, testing often only takes place in the context of the full system, which requires high hardware costs, is only possible late in the development process and leaves little scope for variant investigations and detailed characterisation of the individual substructures. Hybrid testing methods enable faster, meaningful testing of such substructures through simulation-based optimised test designs. These hybrid methods combine numerical and experimental procedures in one testing process. These include hardware-in-the-loop methods, the use of digital twins of test setups and the simulation-based determination and optimisation of variable quantities in the respective test [1]. The latter group of hybrid testing methods also includes the derivation of test designs in which numerical analyses are used to optimise attachment and load boundary conditions in such a way that the simplest possible test setup with the most accurate possible damage reproduction is achieved for the respective test task. Examples of such test approaches and various applications can be found in the literature, for example in [2]-[7].

3 Procedure for the systematic derivation of optimised test designs

For the optimisation of test designs regarding complexity and information quality, a numerical model of the complete system under service loading and a model of the substructure to be tested are required. Typically, FE models are used for this purpose. The reference stresses are determined using the model of the complete system under service loading. The test boundary conditions are optimised using a model of the substructure. Due to the computing time, this optimisation cannot usually be realised with direct use of the FE models, as the number of parameters would require several thousand simulation runs. The process shown in fig. 1 enables efficient optimisation, whereby numerous design variants of the test setup are evaluated.

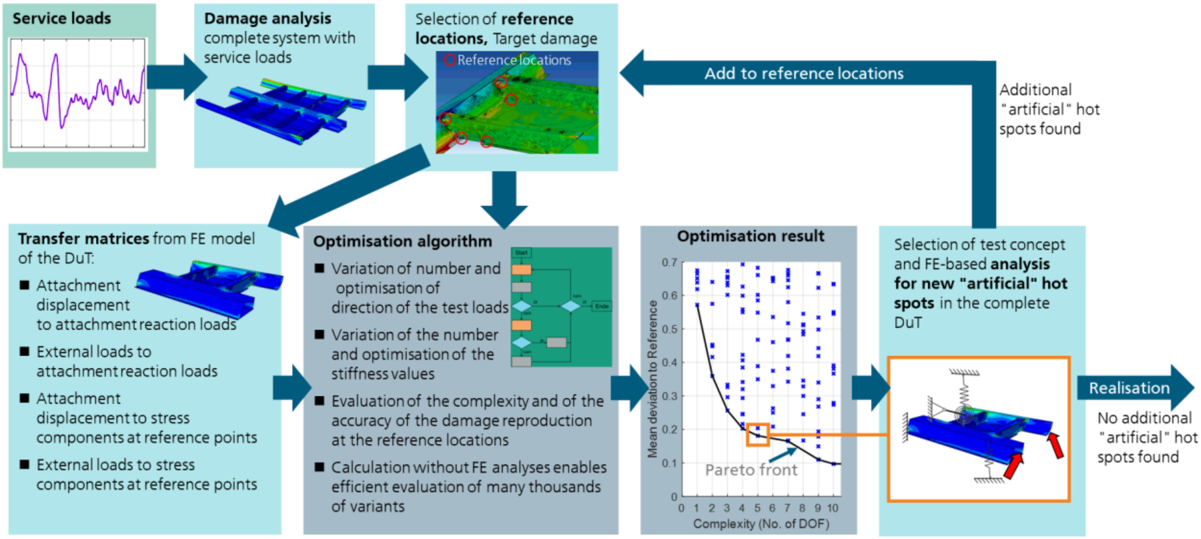

Fig. 1
Procedure for optimising the substitute test.

To do this, possible hot spots must first be identified using the reference model of the complete system and the target quantities for optimisation need to be limited to the stresses at these reference locations. Transfer matrices can be exported from the FE model of the Device under Test (DuT), which can be used to describe the stress components at the reference locations as a function of the external test loads and the elastic attachment boundary conditions. This requires the stiffness matrix of the DuT in relation to the degrees of freedom of the attachment, the transfer matrix of the test loads to the reaction forces at the attachment (with ideally rigid support in the degrees of freedom of the attachment), as well as the transfer matrices of the deformation variables (displacements, rotations) at the attachment locations and the test loads to the local stress components at the reference locations. With these transfer matrices and suitable evaluation methods, the influence of each change in the elastic attachment conditions and the test loads on the local stress can be evaluated in just a few seconds. The optimisation algorithm systematically varies the test loads and the attachment conditions, e.g. by neglecting load channels and elastic attachment boundary conditions or by varying load directions and attachment stiffnesses. The transfer matrices can be used to determine the time histories of the stress components for each variant. Finally, the influence of the changes on the local damage at the hot spots compared to the reference damage is evaluated. The optimisation algorithm provides the solution with the highest replication accuracy regarding the damage at the reference locations for all degrees of complexity examined in the solution space, whereby the degree of complexity results from the number of load channels considered in the test variant and the number of elastic attachment boundary conditions. As a result, the optimisation delivers a Pareto front of possible solutions, in which each solution offers either a lower complexity or a higher accuracy compared to every other solution in the Pareto front. The solution that represents the best compromise regarding the respective test objectives is then selected from these solutions. As the optimisation only takes place regarding the selected reference locations, the entire test specimen structure must finally be evaluated with the selected solution to rule out the possibility of the planned simplifications leading to new, "artificial" hot spots that would only occur due to the simplification of the test setup. If such artificial hot spots are found, these locations must be considered as additional reference locations in the optimisation and the optimisation must be repeated including them. If no artificial hot spots are found in this check, the optimised test concept is implemented.

4 Application examples for hybrid testing methods

In this section, the attachment of a light truck battery and a structurally integrated high-voltage storage system are described as examples to show how hybrid testing methods enable simplified component and structural testing.
For components that are connected to the truck frame at several points, like the truck battery shown in fig. 2 (left hand side), frame deformation has an important effect on the local stresses. On the right-hand side of fig. 2 a simplified test bench for the battery frame attachment is depicted, which has been derived using the process described in section 3. Instead of the entire truck frame, on which there are 35 load application points, only the frame section in the vicinity of the battery is tested in the simplified test concept. This section is loaded with three uniaxial forces: one at the front end of the longitudinal

member, one at a platform connection point near the battery and one at the centre of gravity of the battery replicating inertial loads.

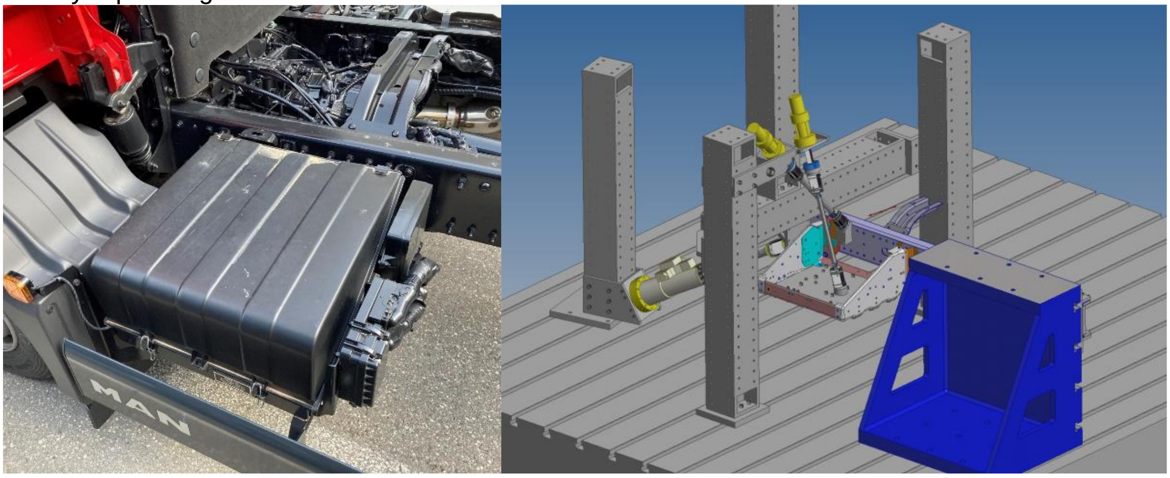

Fig. 2
Battery box connected to the frame of a 12-t light truck (source: MAN) (left-hand side) and substitute test designed for this its attachment to the truck frame (right-hand side) [7].

For the frame section under test, the load vectors at the three load application points were optimised regarding damage-equivalence. This optimisation was carried out for various possible frame sections. The choice of this section has a significant influence on the flow of forces and thus on the local damage.
Hybrid testing methods are also interesting for segments from larger complex structures [1]. Fig. 3 shows a test setup for a segment of a car high-voltage storage (HVS) system integrated into the vehicle floor.

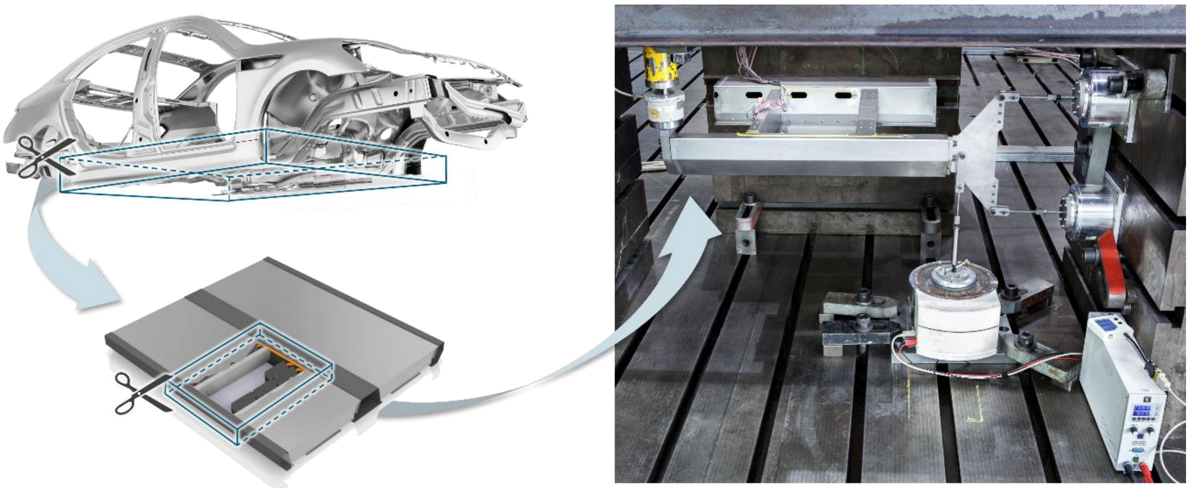

Fig. 3
Simplified test for a segment of a car high-voltage storage system integrated in the vehicle floor with three adjustable mounts as test boundary conditions.

In the example, the structure of the HVS system is integrated into the vehicle floor. In a simplified test only a segment of the HVS structure is tested. The focus of the test is the realistic testing of various innovative joining processes on this segment, which were developed in the "Light Materials for Mobility (LM4M)" project at Fraunhofer. Mounts with adjustable stiffness prototypically realised by Fraunhofer LBF [8, 9] are used in this test rig. These can be used to emulate different stiffnesses of the surrounding car body structure.
The stress in the structure can be significantly influenced by specifically adjusting the stiffness of the mounts. This makes it possible to realise a test for different installation situations of the structure with one test rig by adjusting the stiffness of the mounts, which correspond to different vehicles or vehicle variants.

5 Conclusions

Hybrid testing methods are an important tool for verifying and optimising fatigue strength in an efficient product development process. They can be used to test substructures and components characterised by significant interactions with adjacent structures, without including these adjacent structures. This enables testing under the real stresses to which they are also subjected in the complete system at an earlier stage in the development process. This avoids lengthy and expensive modifications due to weak points that are only discovered at a late development stage. Instead, it enables earlier lightweight design optimisation as well as more extensive variant investigations and component characterisations than is possible when testing in the complete system. Such an approach combines the advantages of numerical and experimental methods in the testing process. Today, numerical simulation can model the external loads and internal stresses of the structures with sufficient accuracy. They can be transferred to simplified tests in a realistic manner using the methods described. However, the actual component-related material strength can still only be determined with sufficient certainty in experimental testing.

6 References

[1] Landersheim V., Hansmann J., Bartolozzi R., Millitzer J.: „Hybrides Testen - Verbindung von numerischer Simulation und experimenteller Prüfung zur Steigerung von Genauigkeit und Effizienz“, DVM Workshop Prüfmethodik für Betriebsfestigkeitsversuche in der Fahrzeugindustrie, May 4/5 2022, Sindelfingen

[2] Walter M., Gorgas S.: „Virtuelle Prüfstandsdefinition zur realitätsnahen Prüfung nicht entkoppelter Achsträger“, Materials Testing: Vol. 49, No. 9, pp. 480-486, 2007

[3] Kiesel A., Schliebner R., Seise M.: „Entwicklung und Anwendung von mathematischen Optimierungsmethoden zur Ableitung von vereinfachten Prüfungen für Fahrwerksbauteilen“, Materialwissenschaft und Werkstofftechnik, Vol. 42, No. 4, pp. 306-313, 2011

[4] Soproni I., Lindtner E., Franschitz S.: “Load and Fatigue Life Equivalent Reduction of Component Tests from Road Load Data for Efficient Part Validation”, International FEMFAT User Meeting 2013, May 15 - 17, Steyr, Austria

[5] Landersheim V., Möller R., Dittmann K.-J.: „Ableitung Eines Vereinfachten Ersatzversuchs Für Pkw-Integralträger Mittels Numerischer Schädigungsbewertungen“, 43. Tagung des DVM Arbeitskreises Betriebsfestigkeit: Potenziale im Zusammenspiel von Versuch und Berechnung in der Betriebsfestigkeit, Steyr, Austria, October 12/13 2016

[6] Lozia Z.: “The concept of the application of modelling and simulation to simplify and reduce the cost of durability tests of vehicles and their components”, The 13th International conference on Automotive Safety, 2022, doi:10.1088/1757-899X/1247/1/012011

[7] Landersheim V., Küppers M.: „Ansatz zur Betriebsfestigkeitsbewertung der rahmenseitigen Anbindung von Energiespeichern mittels Ersatzversuch auf Basis numerischer Schädigungsanalysen“, 48. Tagung des DVM AK-Betriebsfestigkeit: Betriebsfestigkeit – Wissensmanagement und Methodenentwicklung entlang der Wertschöpfungskette, October 12/13 2022, Plauen

[8] Millitzer J., Hansmann J., Lapiccirella G., Tamm C., Herold S.: “Tuning and Emulation of Mechanical Characteristics - Tunable Mounts and a Mechanical Hardware-in-the-Loop Approach for More Efficient Research and Testing” In: Pelz, P.F., Groche, P. (eds) Uncertainty in Mechanical Engineering, ICUME 2021, Lecture Notes in Mechanical Engineering. Springer, Cham. doi: 10.1007/978-3-030-77256-7_12

[9] Hansmann J., Seipel B., Kaal W., Kraus R., Melz T.: „Vorrichtung zur Übertragung oder Entkopplung von mechanischen Schwingungen (EP2694836B1)“, European Patent Office. https://worldwide.espacenet.com/patent/search/family/045562264/publication/EP2694836B1?q=pn%3DEP2694836B1, 2018

Creating Surrogate (Simplified) Loads From Multiple Vibration Environments

Neil Bishop (Hexagon), Philippe Leisten (Purem GmbH)

.

1 Background & Introduction

A common challenge in durability analysis is to reduce measured (multi event, multi component) vibration data samples into a single surrogate load specification. This is usually done so that new design proposals can be evaluated either in a test situation or a virtual analysis. Historically enveloping has been used for this task. Enveloping is the name given to a process where the maximum value of a series of PSD's is retained as the envelope. The downside of enveloping is that the test specification tends to be very conservative. By definition, the envelope is the maximum (worst) for all cases. This presentation introduces a new procedure which should generate more realistic specifications.

2 Proposed New Procedure

The following process for deriving Surrogate Loads has been implemented

,

- Step 1: Calculation of Pseudo Damage channel factors in the Time Domain (PDTD) for multi event loads - fully automatic.
- Step 2: Time2PSD reduction of multi event, multi channel, time histories into PSD envelopes (1 per channel).
- Step 3: Calculation of Pseudo Damage channel factors in the Frequency Domain (PDFD) using envelopes – semi automatic.
- Step 4: Scaling of the channel envelopes to create single channel Surrogate Loads in the following way:
  Scaled channel Surrogate Load = PSD Envelope * PSDT/PSDF. Note that this scaling currently has to be done manually.
- Step 5: Calculation of a single diagonal PSD Matrix (Surrogate Load) calculated using these channel envelopes * PSDT/PSDF.

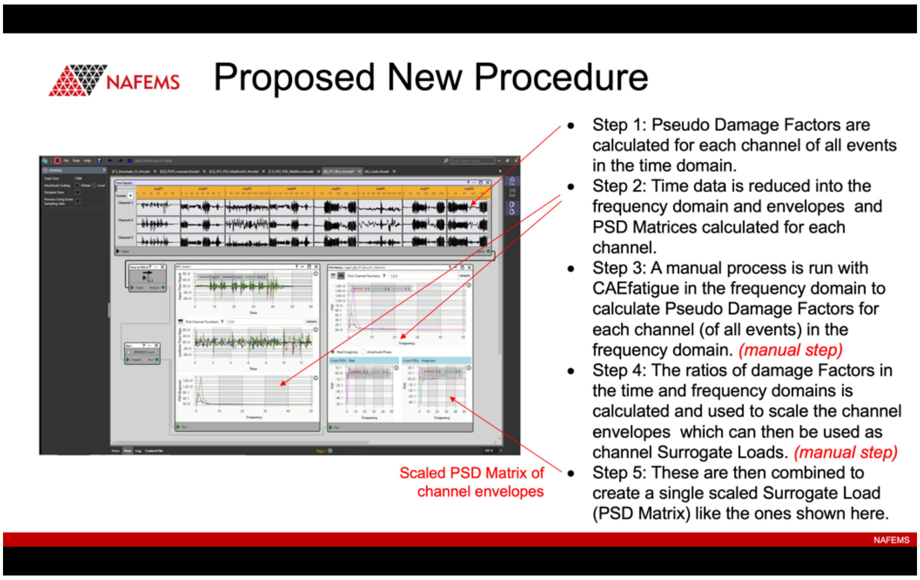

This new approach should result in more accurate and less conservative loads for future designs and should be used by designers needing loads for future designs based on legacy design loads. The CAEfatigue software contains all the required files to fully implement the above process.

3 Summary of Results and Discussion

Actual damage with correlated loads:	***10.57***
Actual damage with uncorrelated loads:	***15.50***
Damage with individual channel Surrogate Loads:	***5.60***
Damage with uncorrelated PSD Matrix Surrogate Loads:	***22.06***
Damage with correlated PSD Matrix Surrogate Loads:	***???***

We have not yet completed the process of creating a correlated PSD Matrix Surrogate Load (this is currently being worked on). So the best comparison that can be made is between ***22.06*** (Surrogate Load damage uncorrelated loads) and ***15.50*** (actual damage uncorrelated loads).

This is a very close result (conservative by a factor 1.42) and acceptable as a difference. Once the correlated Surrogate Load is available that comparison will also then be made.

When applied separately as channel loads (base shake separately in the X, Y and Z directions) the damage obtained is 5.60 (unconservative by factor of 0.36). This is understandable because, although the X and Y damages are low, when added to the Z loading, they have a very significant affect.

4 Future Work

This presentation has described the first implementation of a new technique for calculating simplified (Surrogate) loads.

In this first release only an uncorrelated Surrogate Load is shown and there are several manual steps.

It is expected that in the next release a fully automated Surrogate Load version will be developed.

It is also expected that in the next release a method for including correlation in the Surrogate Load will be developed.

5 References

[1] CAEfatigue User Guide Examples, Hexagon 2024

Fatigue Strength in Hydrogen Applications – Current Applications and Trends

Dirk Rensink

Segula Engineering)

Fatigue design simulation of mechanical equipment including seven case studies

Rob Widders

Consultant, Sydney Australia

1 Summary

1. This short webinar outlines the recommended processes for overall and detail fatigue design simulation of mechanical equipment to reduce the potential for the occurrence of fatigue cracking damage in operation – hence resulting in a more durable and reliable plant item.
2. Outlined in each step are the suggested actions to be taken, and the standards and reference documents to be followed. This ensures that all required steps are followed to deliver a more durable product to address design for fatigue loading.
3. Seven case studies are included. The webinar details the 3D geometrical form of the equipment, particularly at inherent stress concentration joints and transitions, which are needed to suitably accept the loading conditions, by providing acceptable joint design, structural continuity and load paths in a holistic design manner. The seven case studies are some of the many the author has been involved in as a principal engineering consultant, summarising the design shortcomings, where the fatigue issues occurred, and what the design rectification solutions were. It is trusted that the text will be of use to graduate as well as more senior engineers in the need for good fatigue design simulation practices.
4. The fatigue design simulation methods are also summarised, specifically in the use of computational finite element methods and correlation of the outputs with the typical fatigue analysis standards BS7608 (Ref 2) and the numerous IIW fatigue codes (ref 5, 6, 10, 14). Iterations of the simulation and design processes must be completed to result in a fit for purpose design solution of required operational life.
5. The webinar has not been compiled from a metallurgy or materials science basis – rather a practical mechanical engineering design basis. The case studies only involve fabricated mechanical equipment – either steel or aluminium. Mean stress influences are referenced, but not discussed.
6. The 20 minutes webinar timing means that some of the slides will be quickly passed over – all slides are included for relevant later perusal. The case studies and associated schematics span from the 1980s to late 2010s – obviously some schematics from earlier in this time period very clearly reflect that – the learnings from them are the key.

2 Chapter

1 Introduction

2 Context, Codes, Consequences
Case study 1 – ore grinding mills

3 Typical machine loading cycles
Case study 2 – vibrating screens

4 Fatigue Design Philosophies
Case study 3 – centrifugal fans

5 Fatigue Design Recommendations

6 Design verifications – FEA and fatigue analysis to BS7608:2014

7 Post weld fatigue improvement
Case study 4 – ship structure
Case study 5 – dump truck tray

8 Low – mid cycle fatigue (strain life), multi-axial fatigue
Case study 6 – lifting lugs

9 Design validation aspects
Case study 7 – agitator

10 References (5 pages, 40 refs)

3 Learnings

The webinar aims to assist attendees to achieve a suitable engineering practice based understanding of the nature of fatigue loadings, how and why they are usually very damaging to mechanical equipment and plant subjected to them, and the design / verification / validation skills and techniques needed to ensure such equipment and plant can withstand these loadings over a suitably long design life. The webinar will not be written from a metallurgy or materials science basis – rather a practical engineering design basis.

Key takeaways from this webinar are:

- Gain a practical understanding of the fundamentals of good design and simulation analysis for mechanical equipment across a range of mechanical equipment and plant. Seven case studies are included.
- Learn the nature and application of the critical sequential and iterative steps in the combined fatigue design / simulation process so that none are missed, all are applied in the correct order and with the required intensity, so that product function, quality, durability and integrity results.
- Become aware of the nature of fatigue loadings – low cycle, medium/high cycle, cumulative fatigue – rainflow analysis, cycle and damage histograms.
- Gain exposure to the fatigue loading operational conditions of numerous heavy industry mechanical equipment and plant types, so that such knowledge can be applied in their own day to day design, simulation, fabrication, and maintenance activities.

4 References

1. Metso.com
2. BS7608:2014 “Guide to Fatigue Design and Assessment of Steel Products”.
3. ASM International 2008 Ch14 Fatigue.
4. Generation and use of standardised load spectra and load-time histories Article in International Journal of Fatigue. August 2005 Heuler, Klatschke.
5. IIW document IIW-1823-07 ex XIII-2151r4-07/XV-1254r4-07 December 2008 RECOMMENDATIONS FOR FATIGUE DESIGN OF WELDED JOINTS AND COMPONENTS. Hobbacher
6. IIW International Institute of Welding (IIW), XIII-2460-13 – “Recommendations for Fatigue Design of Welded Joints and Components, 2013”. (2nd ed 2014)
7. Metal Fatigue in Engineering. 2nd ed. Stephens, Fatemi, Stephens, Fuchs. 2001.
8. Multiaxial Fatigue. Socie, Marquis. 2013.
9. Fatigue assessment of welded joints by local approaches”. 2nd edition 2006. Radaj, Sonsino and Fricke.
10. IIW 2018 document “Structural Hot-Spot Stress Approach to Fatigue Analysis of Welded Components. Designers Guide. Niemi, Fricke and Maddox.
11. Introduction to metal fatigue. Mechanical Engineering Technical Report ME-TR-11 M M Pedersen. 2018

12. Benchmarking Newer Multiaxial Fatigue Strength Criteria on Data Sets of Various Sizes. Papuga, Nesládek, Hasse, Cízová and Suchý. MDPI 2022.
13. Fatigue Design of Process Equipment ASME Plant Engineering & Maintenance Technical Chapter March 12, 2009. Hinnant Paulin Research Group
14. AS1554.5 Structural steel welding. Welding of steel structures subject to high levels of fatigue loading
15. International Institute of Welding. Best Practice Guide on Statistical Analysis of Fatigue Data. C R A Schneider and S J Maddox. 2003.
16. www.rud.com.au
17. CAEFatigue (Hexagon) https://hexagon.com/Products/Product-Groups/computer-aided-engineering-software/CAEFatigue
18. FE-Safe (3DS) https://www.3ds.com/products-services/simulia/products/fe-safe/fe-safe/
19. nCode https://www.ncode.com/
20. Cidect Construction with Hollow Steel Sections Design Guide 8 – "For circular and rectangular hollow section welded joints subject to fatigue loading". 2001.
21. SAE Fatigue Design Handbook.
22. The site www.efatigue.com has many useful folders.
23. This document has good background on weld quality; https://link.springer.com/content/pdf/10.1007%2Fs40194-017-0490-5.pdf
24. Niels Ostergaard mechanics lectures; https://www.hochschule-rhein-waal.de/en/faculties/technology-and-bionics/organisation-and-office-hours/professors/prof-dr-niels-ostergaard
25. VDI 2230 Systematic calculation of high duty bolted joints
26. ASTM E1049 Standard Practices for Cycle Counting in Fatigue Analysis
27. Ship Performance under Multiaxial Loading. SSC-356. 1990.
28. Validation of Multiaxial Fatigue Strength Criteria on Specimens from Structural Steel in the High-Cycle Fatigue Region. František Fojtík, Jan Papuga, Martin Fusek and Radim Halama. MDPI 2021.
29. Hot spot stress assessment at fillet welded joint using different finite element weld modelling techniques and its validation. R Chillal, N Pagar. WJERT, 2016, Issue 5, 270-290.
30. Stress Analysis and Fatigue of Welded structures. G Glinka, M S El-Zein, R A Formas. Welding in the world, July 2013.
31. Procedural Benchmarks for Common Fabrication Details in Plate/Shell Structures. NAFEMS Publications, March 2005, ISBN-13-1874376026.
32. Atlas of Fatigue Curves. Editor HE Boyer. ASM International.
33. Welding in the World. Vol 57 2013.
34. On the interaction of axial and bending loads in the weld root fatigue strength assessment of load-carrying cruciform joints. A Ahola · R Hamidreza · T Björk · O Kukkonen Welding in the World (2022) 66:731–744
35. FKM-Guideline. Analytical strength assessment of components in mechanical engineering 5th edition. 2003. English Version Translation by E. Haibach
36. Investigation of fatigue assessments accuracy for beam weldments considering material data input and FE-mode type. Yevgen Gorash et al 2017 J. Phys.: Conf. Ser. 843 01202
37. Effect of increased yield strength, R-ratio, and plate thickness on the fatigue resistance of high-frequency mechanical impact (HFMI)–treated steel joints M. Leitner & Z. Barsoum Welding in the World 2020 64:1245-1259
38. Influence of the mean stress on the fatigue life of welded joints under variable amplitude loading Xu Liu, Yan-Hui Zhang, Bin Wang, Xing Sun. International Journal of Fatigue. 163 (2022)
39. https://community.sw.siemens.com/s/article/mean-stress-corrections-and-stress-ratios
40. API 684 Tutorial on the API standard paragraphs covering rotor dynamics and balancing; an introduction to lateral critical and train torsional analysis and rotor balancing. 2019.

Fatigue Simulation Software from Engineers for Engineers

Axel Werkhausen

Magna Powertrain Engineering Center Steyr GmbH & Co KG

FEMFAT is developed in Engineering Center Steyr- a company, meanwhile belonging to MAGNA and so has first class reputation all over the world in automotive engineering and excellence. The software started with simple routines and coding on 6 different hardware platforms and operating systems to satisfy the customers needs down in 1986. Over the years, automotive industry is no longer the solely customer for fatigue analyses in FEMFAT.

The spread of users also increases the requirements in materials, interfaces, simulated production processes and in some ways also the fulfillment of regulations like the Germanischer Loyd for wind energy gearboxes. FEMFAT combines the positive ideas for fatigue analyses from the different mechanical engineering tasks and offers the simulation engineer a wide variation of not only useful, but comfortable to use simulation tool.

The presentation will showcase the process of how to improve the engineering skills from a simple fatigue analysis of a specimen to correlate the material data of a hardened shaft to the final use case when this shaft is part of the drive shaft joint. Such drive shaft joint has to withstand the loading from different inclination between driveshaft and differential, but any combination of different torque in reasonable time and with today's workstations to make it affordable to every engineer in this business.

The tool, that enables the multitude of load cases in reasonable time once has been developed for the fatigue simulation of hyper elastic natural rubber in an engine mount. The engineering skills of about 100 MAGNA simulation engineers and thousands of simulation engineers at the FEMFAT customs and universities enlarge the capability of engineering software packages by challenging the software and requesting new features to be implemented. That`s part of our plan for development and benefits the FEMFAT-community.

Fatigue Life Analysis as Part of the Design Optimization Process for Welded Structures

George Korbetis, Ioannis Karypidis, Christos Tegos (BETA CAE Systems)

1 Summary

Product design in the automotive industry is becoming increasingly demanding as new products should reach high performance standards in very short development cycles. Engineering simulation, using FEA, comes to assist in most product development stages to substitute costly experiments for new designs while speeding up the overall processes. In this direction, optimization procedures are increasingly employed during the design.

Apart from FEA, fatigue analysis is a mandatory process which assures product integrity by accurately predicting products' life. Using fatigue analysis, the engineer is able to construct stronger yet lighter structures while avoiding overdesign. Special attention should be paid to welded structures since welds often are the weakest part concerning the fatigue life.

Fatigue analysis is often incorporated into the product design workflow through an optimization process that fine-tunes structures' efficiency.

In this case study, a subframe of a car is subjected to a cyclic load. Several design variables are defined directly to the assembly's FE model to control its shape. The fatigue analysis as a part of an optimization loop analyzes the model and locates critical areas for improvement.

2 Problem set-up

The target of this case study is to perform design optimization on a sub-assembly of a car model. The goal is to reduce fatigue damage while keeping mass and stress within specified limits. The fatigue analysis focuses on seam-welds, as these are the most vulnerable areas. The input load for the case is calculated by running the car's kinematic model on a Belgian block road. All actions required for this task are set up automatically so they can run in an optimization loop. These actions are described in the following sections.

2.1 Design changes

The selected sub-assembly is subjected to several shape and gauge changes. Areas of high stress are selected for shape modification where high damage is likely to occur. Additionally, some non-critical areas are selected which can possibly contribute in mass reduction. These changes are applied directly to the FE model using the ANSA morphing tool, eliminating the need for remeshing or updating the FE model. For the seam-welds, the length is set as a design variable. The seam-weld connection is realized after modifying its length to avoid shape distortions on the connection elements. Twenty-three design variables are defined to control geometrical changes, seam-weld lengths, and sheet metal thicknesses. Figures 1 and 2 show the sub-assembly and some of the shape modifications.

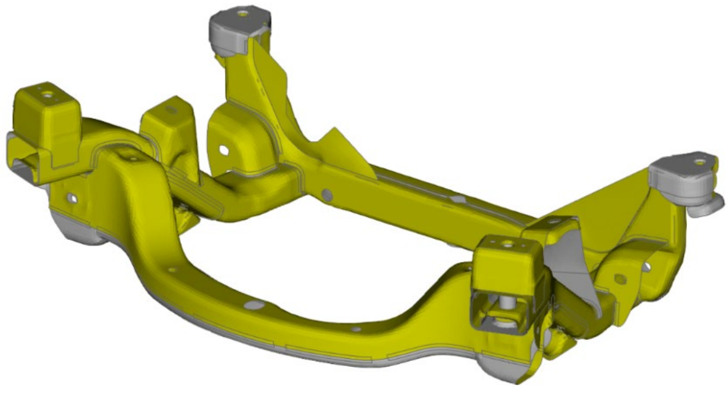

Fig. 1
The sub-assembly

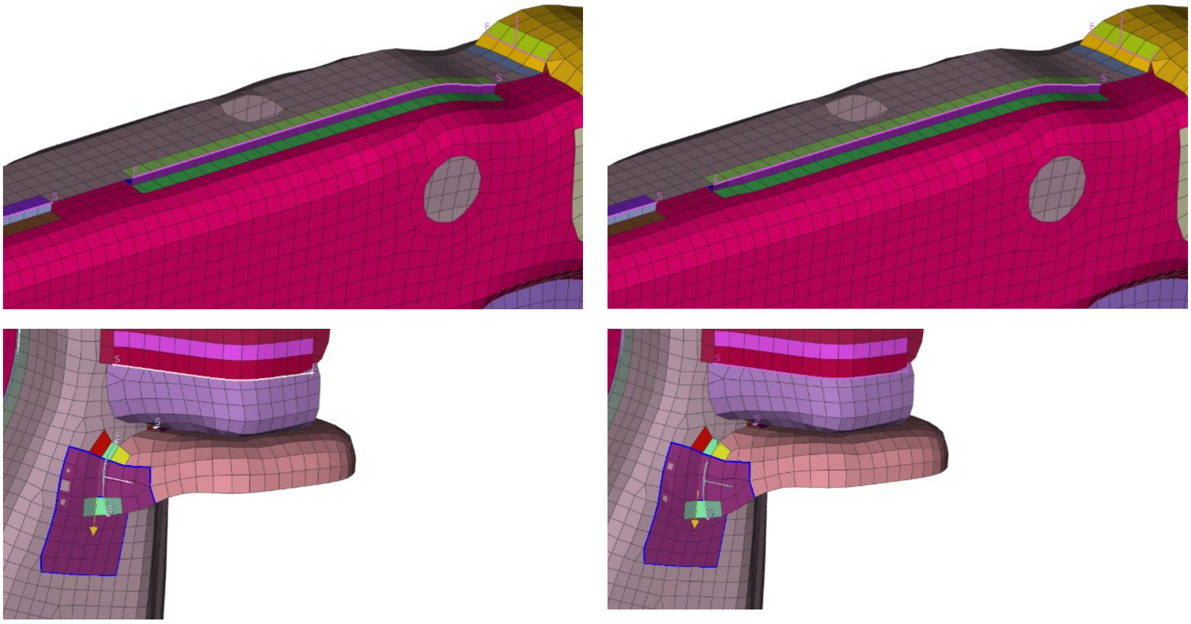

Fig. 2
Shape changes on the FE model

2.2 The Kinetics model

The kinetics model is derived from the car's FE model (Fig. 3). All bodies are considered rigid except for the subframe assembly, which is treated as a flexible body. An eigenvalue analysis is applied to the flexible body to calculate the stiffness matrix and eigenmodes. The car is then run on a Belgian block road for ten seconds, and the ANSA Multi Body Dynamics solver calculates the dynamics of the entire assembly, as well as the modal stresses and displacements on the subframe assembly (Fig. 4).

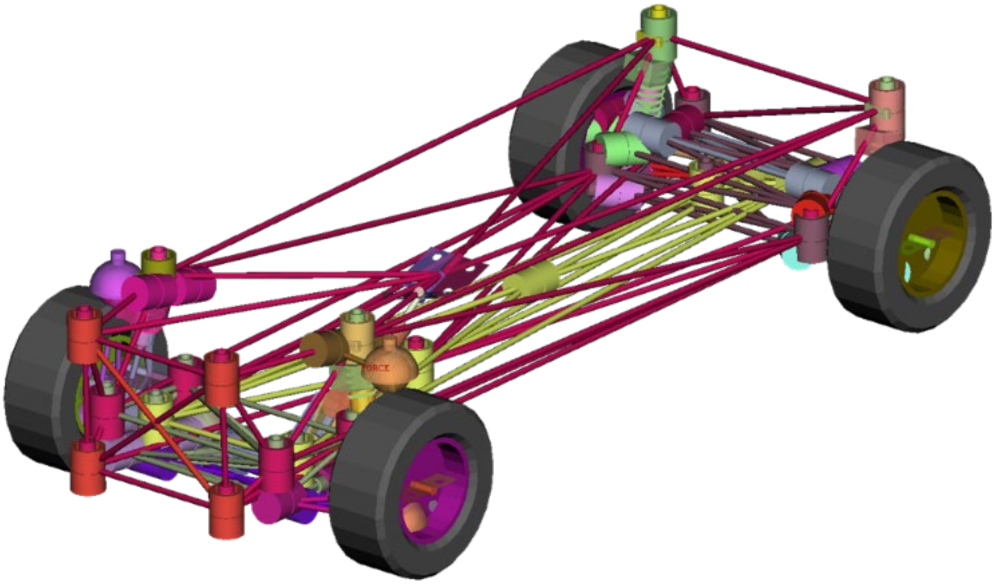

Fig. 3
The kinematics model

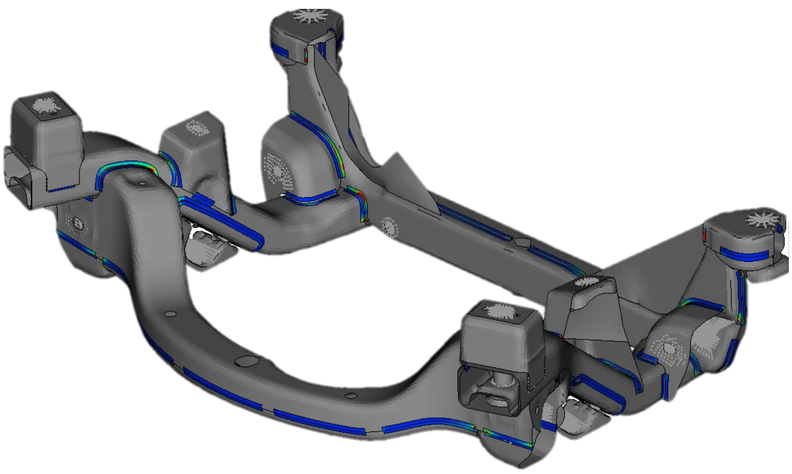

Fig. 4
The flexible body

2.3 Fatigue calculation

The fatigue analysis is performed using the FATIQ software (Fig. 5). The input data for this analysis consists of the modal stresses and displacements of the subframe, computed from the kinematic model. Damage calculation is carried out by first combining the modal displacements and stresses to produce transient stresses. In the second step, Miner's rule is applied to cycles extracted through the Rainflow counting algorithm. The fatigue analysis process has been structured to allow for reuse in batch mode and is coupled with the optimization workflow.

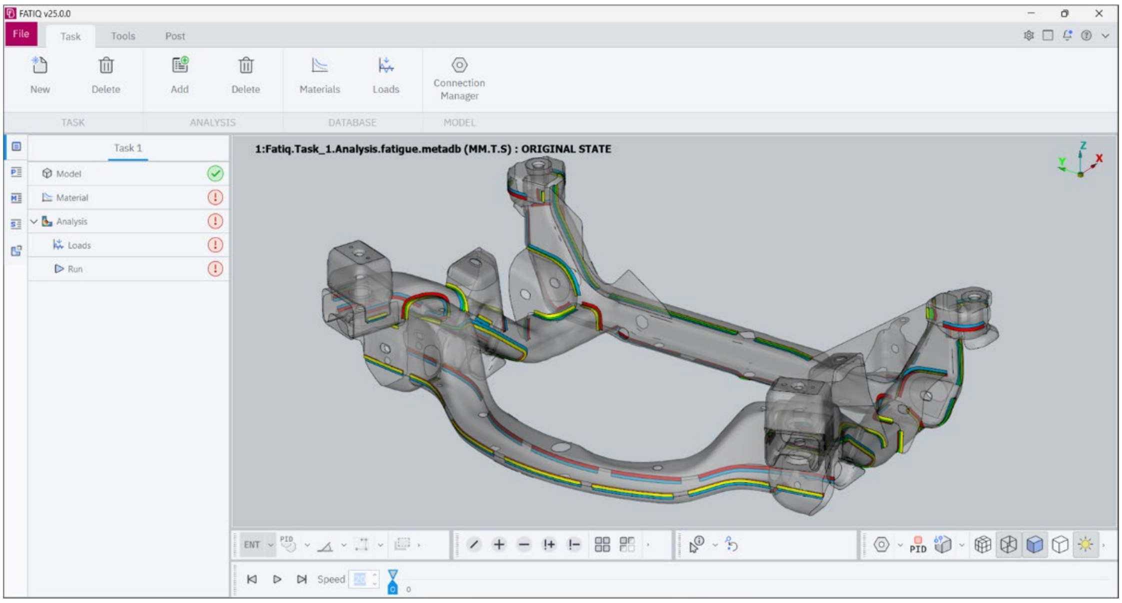

Fig. 5
Fatigue analysis

3 Optimization

The optimization process is conducted in three steps. First, a DoE (Design of Experiments) analysis is performed using all design variables. The responses considered include the maximum damage, the maximum stress, and the mass. One additional response is defined for the total length of all modified seam-welds. This approach allows the optimizer to reduce the length of seam-welds in areas with lower loads. For the DoE, the Uniform Latin Hypercube algorithm is used. Secondly, the created experiments train a Response Surface Model using the Kriging algorithm. Finally, optimization runs on the defined Response Surface Model using the Simulated Annealing algorithm, which converges after twenty-one iterations. A final run of the real model confirms that the RSM is well trained and that the virtual and real optima are close. All the above stages of optimization are defined and run in the ANSA Optimization Tool. The optimization workflow is shown in Figure 6.

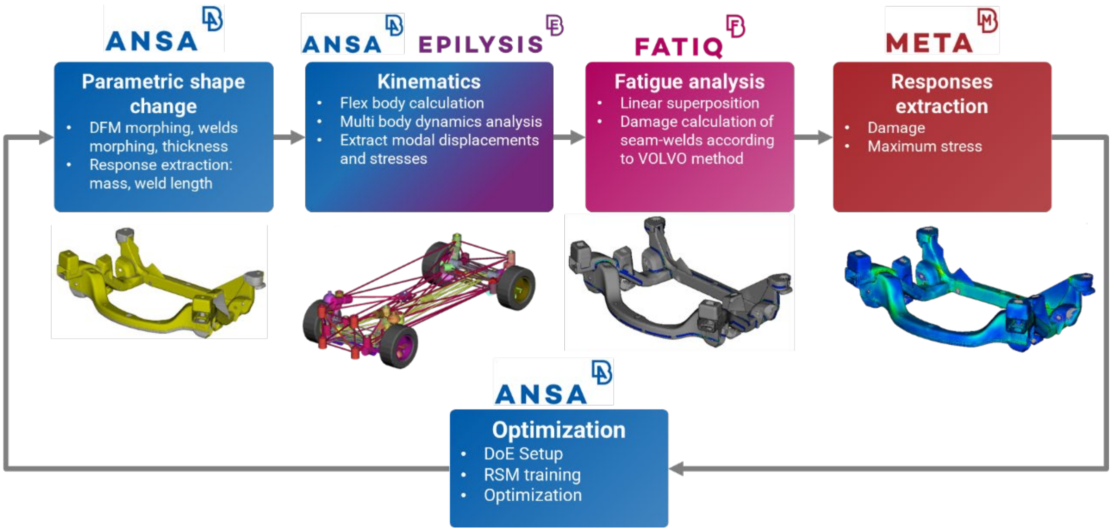

Fig. 6
The optimization workflow

4 Results

A significant reduction in fatigue damage has been achieved while keeping maximum stress and mass within the acceptable range. The shape changes and the objective and response values are shown in Figure 7 and Table 1.

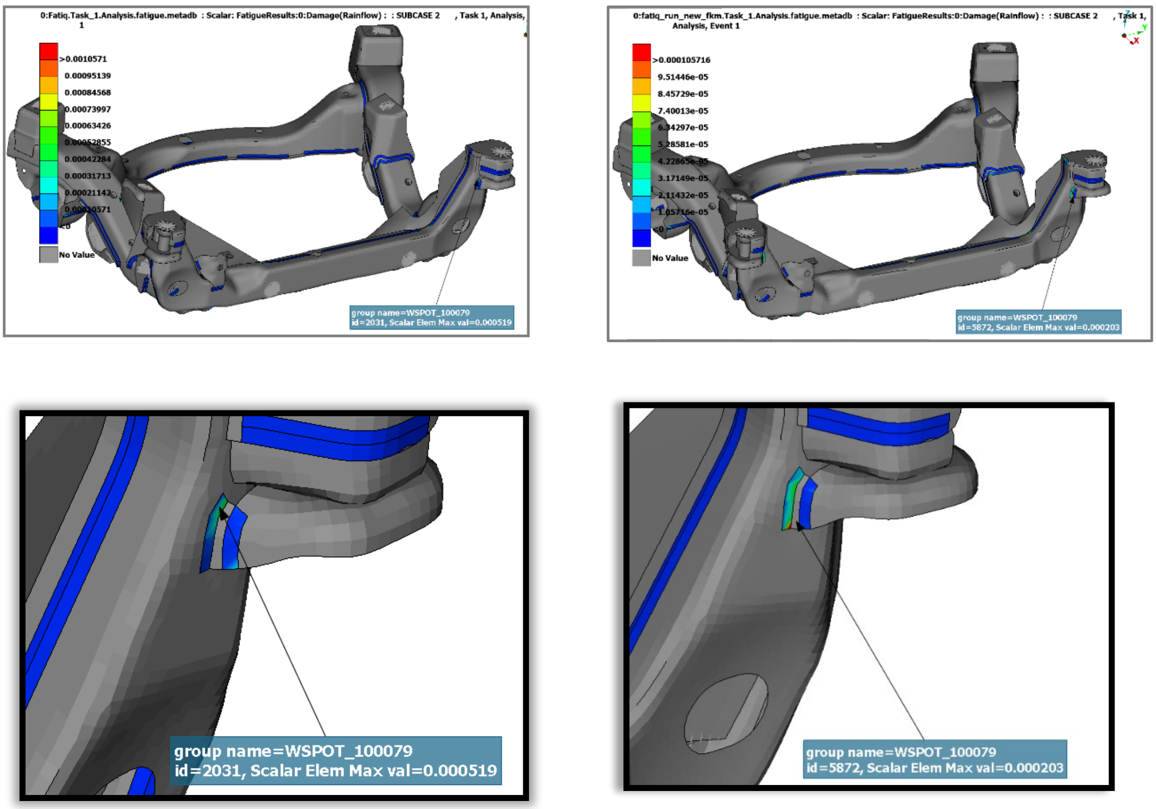

Fig. 7
The initial and final designs

	Initial	Optimum	Difference [%]
Max Damage	0.000519	0.000203	60.7 ↓
Max Stress	492.37	430.34	12.5 ↓
Seam-weld length	698.3	703.6	0.7 ↑
Mass	0.0251	0.0256	1.9 ↑

Table 2
Objective and responses

5 Conclusions

A complex process involving various types of analyses has been seamlessly combined into a single workflow, capable of exploring and optimizing model behavior. The convergence was fast, with a relatively small number of iterations, making it feasible to apply the same process to all critical parts of the car model. This approach can also be extended by using kinematic parameters and fatigue analysis properties as design variables.

Computerized Assessment of Welds based on Finite-Element Analyses

Peter Reimers

IWiS GmbH

Summary:

For a successful assessment of welds in structures subjected to static loads as well as to service loads various conditions have to be accomplished according to the respective standard or guideline. Whilst these conditions may follow different approaches, they have in general in common that stresses in the local weld coordinate system are to be used and that a number of load cases are to be considered.

The calculation of stresses in welded sheet metal structures by Finite Element codes is performed effectively using plate elements. The welds in a construction are usually not explicitly represented by means of elements in order to limit the modelling costs. For a guideline- or standard-compliant assessment, the engineer is therefore faced with the task of not only transforming the stresses calculated in the interconnected metal sheets from the respective element into the local weld coordinate system, but also of calculating stresses in welds that are not present in his model. Furthermore, the required quantities have to be calculated in order to be able to apply the obligatory conditions accordingly.

IWiS has developed a software for this task, supporting the FEA calculation engineer in the weld assessment process. With the aid of this tool, the weld connections are identified automatically in an existing FE model, the required stress transformations are carried out in all elements in the vicinity of the weld connections and the assessment relevant quantities are calculated. Utilisation factors are prepared for a graphic representation in the connected post-processing system as well as summarized in MS-Excel-tables. Thus far weld assessments according to DVS 1612 and DVS 1608, EN 13001 and Eurocode 3 are implemented.

Keywords:

Weld assessment, Fatigue, DVS 1612, DVS 1608, EN 13001, Eurocode 3, WeldFEM, Finite Element Analysis

1 Outline

In general for a structural strength assessment stresses in structures are to be compared with strength values of the applied materials. The way these comparisons are to be performed are specified in standards and guidelines is described in section 2 for the railway industry. Modelling considerations for the calculation of stresses by use of Finite Element Analyses (FEA) are given in section 3. Section 4 explains the determination of assessment suitable stresses in welds on basis of FEA stress results. The derivation of strength values for static as well as for fatigue weld assessments is presented in section 5. The computerized assistance for the weld assessment by IWiS' software tool WeldFEM is described in section 6. An example out of the current practise in the railway industry with assistance of WeldFEM is shown in section 6.

2 Assessment conditions for welds

The applicable assessment conditions for welds depend on the standard or guideline that is usually to be accomplished in the industry branch of concern. Here the assessment process for railway structures will be outlined.

In the German railway industry guidelines DVS 1612 for steel and DVS 1608 for aluminium alloy structures are to be applied (DVS is the German Welding Society).
Stresses in welds are to be assessed for normal- and for shear stress components separately as well as in combination in case of multiaxial stress states.
In detail these conditions are:

$$\frac{\sigma_{\perp}}{\sigma_{\perp,zul}} \leq 1 \quad \textit{(1)} \qquad \frac{\sigma_{\parallel}}{\sigma_{\parallel,zul}} \leq 1 \quad \textit{(2)} \qquad \frac{\tau}{\tau_{zul}} \leq 1 \quad \textit{(3)}$$

$$\left(\frac{\sigma_{\parallel}}{\sigma_{\parallel,zul}}\right)^2 + \left(\frac{\sigma_{\perp}}{\sigma_{\perp,zul}}\right)^2 - \frac{\sigma_{\parallel}}{|\sigma_{\parallel,zul}|} \cdot \frac{\sigma_{\perp}}{|\sigma_{\perp,zul}|} + \left(\frac{\tau}{\tau_{zul}}\right)^2 \leq 1.1 \qquad \textit{(4)}$$

$$\left(\frac{\sigma_{\parallel}}{\sigma_{\parallel,zul}}\right)^2 + \left(\frac{\sigma_{\perp}}{\sigma_{\perp,zul}}\right)^2 + f_v \cdot \frac{\sigma_{\parallel}}{\sigma_{\parallel,zul}} \cdot \frac{\sigma_{\perp}}{\sigma_{\perp,zul}} + \left(\frac{\tau}{\tau_{zul}}\right)^2 \leq 1 \qquad \textit{(5)}$$

(4) applies for steel according to DVS 1612 and
(5) applies for aluminium alloys according to DVS 1608,

with
$\sigma_{\perp}$, the normal stress component perpendicular to the weld,
$\sigma_{\parallel}$, the normal stress component parallel to the weld,
τ, the shear stress and
f_v, a sign factor.

Indices zul indicate the allowable values.
The left hand side terms of the above conditions are referred to as utilisation factors in the following.

3 Finite Element modelling considerations

The calculation of stresses in welded sheet metal structures by Finite Element codes is performed effectively by use plate or shell elements. In order to limit the modelling costs welds in a design are usually not explicitly represented by elements.
In case the FE-model consist also or entirely of 3D-solid elements a weld assessment with WeldFEM is performed by use of stress gauge elements. Stress gauge elements are very thin plate elements that cover the 3D-areas of interest whilst not effecting the results by their stiffness. These elements are detected by WeldFEM and treated accordingly.

Welded joints of sheets are rather modelled by rigid elements closing gaps that arise due to the reduction of 3D-sheets to their midsurface plane or simply by merging the nodes of the elements that represent the joints sheets. Also "glued contact" may be used if available.
Element edge polygons along welds modelled in this way are referred to as weld lines in the following.
Element shapes along weld lines should be as regular as possible, recommended element sizes are 0.7 to 1.4 times the sheet thickness. Overlapping sheets should remain separate and not modelled by elements of combined thickness.

4 Calculation of weld stress components

Stresses as calculated by FEA programs are delivered in element coordinate systems of arbitrary orientation. Therefore for the evaluation of weld assessment conditions these stress components have to be transformed element by element into the coordinate systems perpendicular to the weld in the first place.
As an example the Simcenter Nastran FE code stress components in plate elements are delivered in an element coordinate system as shown in the following figure:

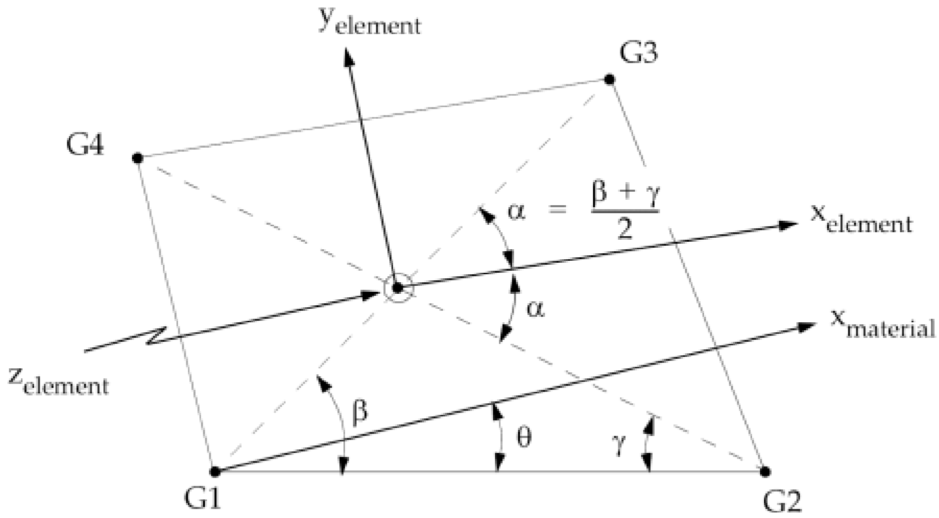

Figure 1: Element coordinate system in NX Nastran 4 node plate elements

Of course any of the element edges may belong to a weld line and each element may belong to more than one weld lines. Therefore the element edge of concern for a given weld line has to be evaluated beforehand and multiple transformation results for a single element have to be dealt with.
The transformed element stress components are then to be converted from the welded sheet into the weld which is not explicitly part of the model. Dividing the weld cross section values "a" by the respectively connected sheet thickness "t" provides a factor $f_w \leq 1$ for each weld-sheet combination. Dividing stress values in the joined sheets by the respective factors f_w provides assessment stresses increased with respect to the stresses in the sheets.
Furthermore the stress augmenting bending influence of a reduced cross section of the weld is to be taken into account for the perpendicular stress component by quadratic extrapolation. Also the strength reduction influence for sheet thicknesses larger than 10 mm has to be considered where applicable.
According to the use of plate stress results element top and bottom stress result have to be evaluated separately.
The guidelines recommend stress evaluation distances off the weld edge. In DVS 1612 this is a measure of 1.0 to 1.5 times the sheet thickness and in DVS 1608 this is 5 mm plus half the size of a strain gage which is usually about 10 mm. As element sizes along the weld line may be smaller than the recommended stress evaluation distances, neighbour elements in the vicinity of the weld line have to be considered in addition to elements directly at the weld line. The according stress transformations have to be performed by adhering to the originating weld coordinate system orientation.
The transformed and converted element stress components are finally to be compared throughout all result sets of concern in order to acquire minima and maxima stress values for the further assessment process.

5 Calculation of strength quantities

For the assessment of stress results for static loading conditions the allowable value is the smaller quantity of R_e / S_e and R_m / S_m. R_e and R_m are the material yield strength and ultimate strength, respectively. S_e and S_m are the respective safety factors against irreversible deformations and rupture. The corresponding shear strength values are determined by division by $\sqrt{3}$.
For the fatigue assessment due to service loads the allowables values are derived from the DVS 1612 MKJ-diagrams for steel or from the DVS 1608 MKJ-diagrams for aluminium in combination with the Haigh-diagram. These diagrams provide allowable fatigue stress values in dependence of the stress ratio R_σ and the mean stress σ_m. Stress ratio R_σ is the quotient of minima to maxima stresses and mean stress σ_m is the arithmetic mean of minima and maxima stresses, each in the respective element for all service load result sets. Figure 2 shows an example for a MKJ-diagram.

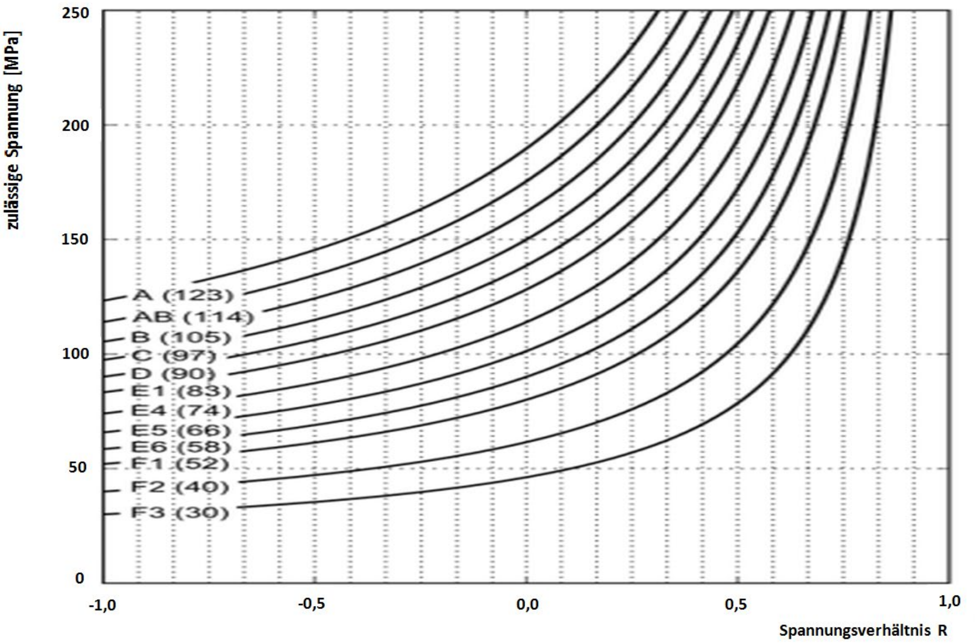

Figure 2: MKJ diagram for steel S235 for normal stresses with positive mean stress.

Upper limits of theses curves are the static strength values. The guidelines provide formulas for the calculation of the different curve slopes. MKJ curves provide allowable minima and maxima in dependence of the stress ratio R_σ whereas the Haigh diagram formulas provide allowable stress amplitudes in dependence of stress ratio R_σ, mean stress σ_m and mean stress sensivities M_σ and M_τ.
The curve to be used for a weld of concern depends on the weld type and the loading state as well as on manufacturing and quality assurance details. The guidelines provide tables with representative examples. An extract of these tables is shown in the following Figure 3 as an example.

The correct choice of the applicable MKJ curve is essential for the assessment.
For service load stresses in the welds an additional factor f_f according to EN 15085 is to be taken into account. For a weld quality class CP C2, where a medium safety requirement and a medium stress state is required, this factor has to be chosen to f_f = 0.9 for example.
Since stress minima and maxima vary from element to element the allowable values are also to be calculated for each element by evaluation of the applicable curve formulas as given in the guidelines.
The calculation of the utilisation factors is finally performed by dividing the converted sheet stress values by the allowable values determined for each element for all load cases of concern.

Tabelle B-1.5. Querbeanspruchte T-Stoßverbindungen, angeschlossener Steg beansprucht.

Nr.	Stoß- und Nahtausbildung					Prüfart und -umfang	Schweißnaht-güteklasse nach DIN EN 15085-3	Kerb-falllinie	Bemerkungen
	Darstellung	Beschreibung	Nahtart	Naht-Nr. nach DIN EN 15085-3	Nahtober-fläche bearbeitet				
1.5.1	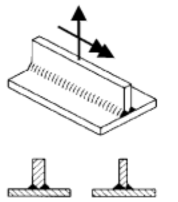	beidseitig durchge-schweißt mit Gegenlage	DHV-Naht HV-Naht mit Kehlnaht als Gegenlage HV-Naht mit Gegenlage	7 10b 10d	ja	10% ZfP-V	CP B u. CP C1	E1+	
1.5.2						Sichtprüfung	CP C2	E1	
1.5.3					nein	10% ZfP-V	CP B u. CP C1	E5+	
1.5.4						Sichtprüfung	CP C2	E5	
1.5.5	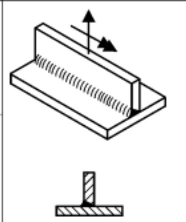	einseitig durchgeschweißt	HV-Naht HV-Naht mit aufgesetzter Kehlnaht HV-Naht mit Badsicherung	10a[3)] 10c[3)] 10e[3)]	nein	10% ZfP-V	CP B u. CP C1	E6	
1.5.6						Sichtprüfung	CP C2	E6-[4)]	
1.5.7	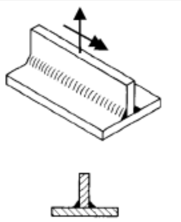	beidseitig nicht durchge-schweißt	DHY-Naht HY-Naht mit Kehlnaht als Gegenlage Doppelkehlnaht	9, 11b 13b	ja	10% ZfP-O	CP B u. CP C1	E6+[1)]	höchstbeanspruch-te Stelle (Anrissort) im Nahtübergang oder an der Naht-wurzel
1.5.8						Sichtprüfung	CP C2	E6[1)]	
1.5.9					nein	10% ZfP-O	CP B u. CP C1	F1+[1)]	
1.5.10						Sichtprüfung	CP C2	F1[1)]	
1.5.11								F2[2)]	

Figure 3: Extract of weld catalogues for the choice of applicable MKJ curves.

6 WeldFEM

IWiS has developed the software tool WeldFEM in order to assist the calculation engineer in the weld assessment procedure. Interfaces for the FE-Systems Simcenter FEMAP by Siemens Digital Industries Software and MSC APEX by Hexagon are currently provided.
In the first place the weld lines are determined automatically for a given FE model that represents the welded structure that is to be assessed.
Weld lines are created by element edges which fulfil one of the following conditions regarding the connection to other elements:
- inclination of more than 75°,
- connection via rigid link elements,
- different material,
- different thickness,
- different element type, e.g. solids.

Exceptions for rigid link spiders are attained automatically, exceptions can also be forced by the user via tagging of property identifiers. Along the detected weld lines dummy spring elements are created for identification in the pre-/post-processing program.
Detected weld lines are given weld types based on thicknesses of the joint plates. As a default fillet welds are presumed with a weld cross section of 0.7 of the smallest connected sheet thickness. According notch types (FAT classes) are chosen in a conservative way. Weld types are open for editing by the user at any time.
Along detected weld lines direct and indirect neighbour elements are gathered for evaluation based on the recommended evaluation distance by the DVS guidelines. The "catch" algorithm for indirect neighbours can be influenced by the user.
Weld lines and neighbouring elements are made available for examination in the connected FE-Postprocessing Software.
Here the automatically detected weld lines can be split and given back to WeldFEM for further editing.

Based on result output sets for static or fatigue loads the according assessment for all welds is carried out as described above. Utilisation factors in all components are calculated for all elements in the necessary weld line vicinity and provided for post-processing in the connected FE-postprocessing system. In addition a MS-Excel File is generated with tables for static and fatigue assessment containing maximum utilisation factors for all weld types for a quick overview.

At present in addition to weld assessments according to DVS 1612 and DVS 1608, standards EN 13001 for welded crane structures and Eurocode 3 for general steel constructions are implemented in WeldFEM.

7 Example

The example as given here provides a short glimpse into the overall assessment process for the battery container of the Zefiro V300 high speed train set.

Figure 4 shows the battery container FE-model.

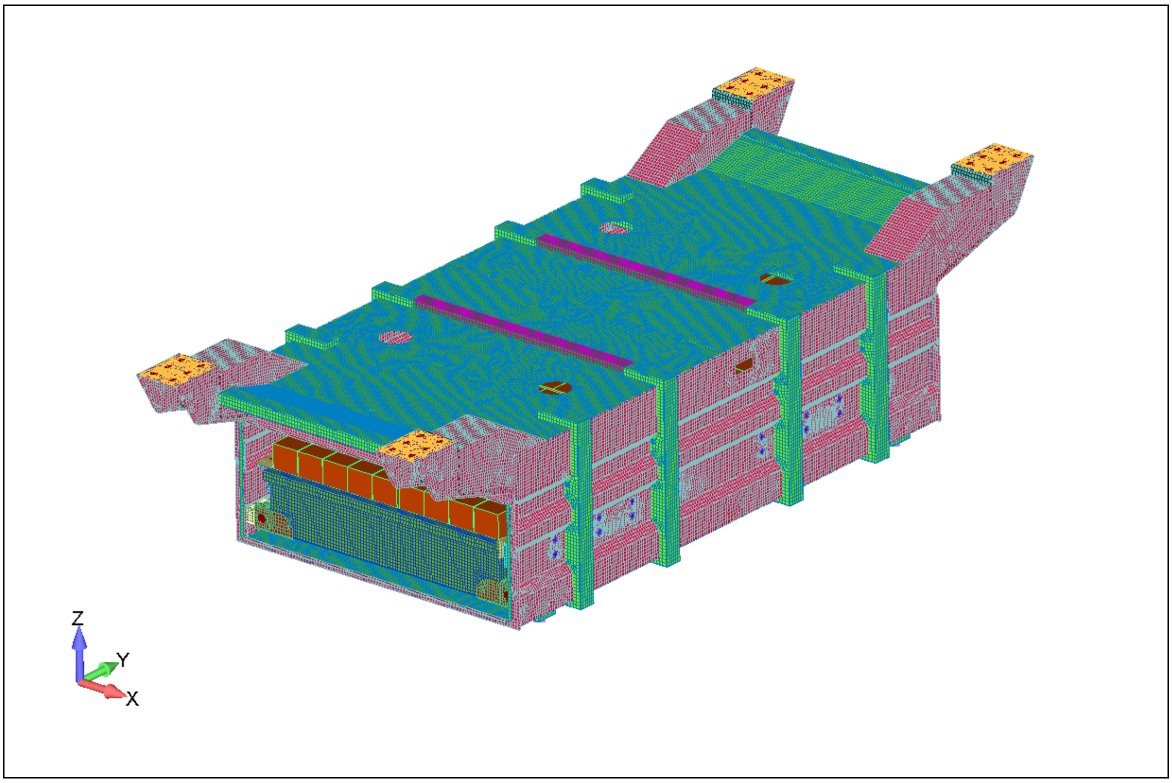

Figure 4: FE-model of the Zefiro V300 battery container.

In Figure 5 the automatically detected weld lines with their neighbouring plate elements are provided.

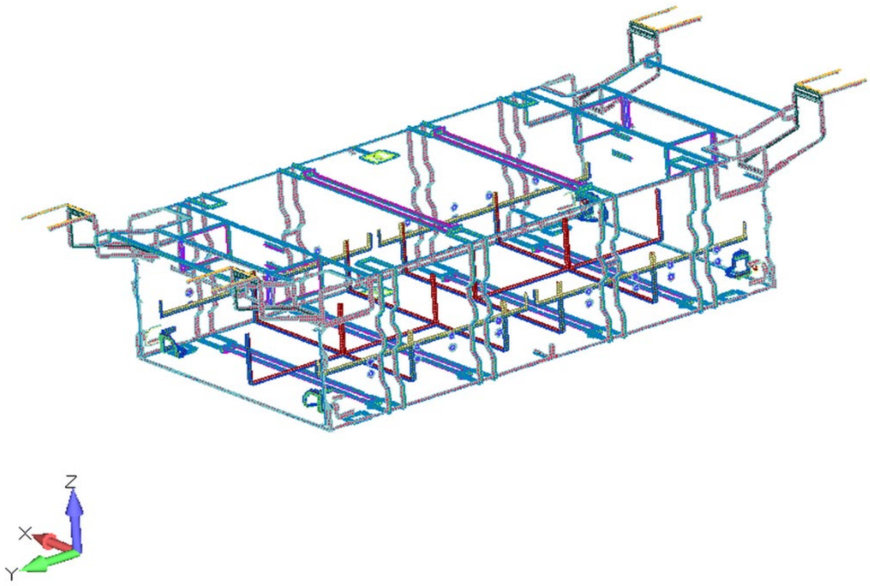

Figure 5: All weld lines and neighbouring elements as detected automatically by WeldFEM.

The post-processing of fatigue utilisation factors perpendicular to the welds for one of the weld types in the container housing is displayed in Figure 6. Here an a2 fillet weld connecting 2 mm with 3 mm sheets is subject of the assessment.

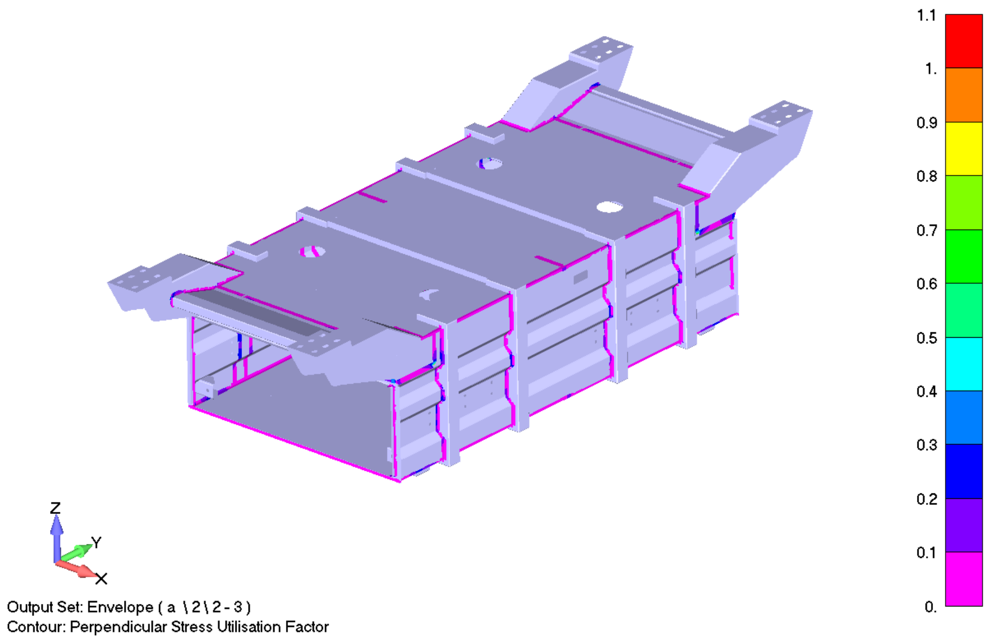

Figure 6: Post-processing of fatigue perpendicular utilisation factors for one of the weld types.

Of course many weld types were to be assessed for the container housing manufactured out of steel S355 as well as for the battery crates out of 1.4301 stainless steel. For each of these weld types all 4 utilisation factors have been examined. For focussing on the critical welds in the design process the tables of maximum utilisation factors for each weld type as provided by WeldFEM were of essential assistance.
A weld assessment in this detail within a reasonable budget and time frame is only to be achieved by computerized evaluation support in the way WeldFEM provides.